

# Lawrence Berkeley National Laboratory

## Recent Work

### **Title**

Preliminary Analysis of Effects of Thermal Loading on Gas and Heat Flow within the Framework of the LBNL/USGS Site-Scale Model

### **Permalink**

<https://escholarship.org/uc/item/221548xx>

### **Author**

Wu, Y.S.

### **Publication Date**

1995-12-01



# Lawrence Berkeley Laboratory

UNIVERSITY OF CALIFORNIA

## EARTH SCIENCES DIVISION

### **Preliminary Analysis of Effects of Thermal Loading on Gas and Heat Flow within the Framework of the LBNL/USGS Site-Scale Model**

Y.S. Wu, G. Chen, and G. Bodvarsson

December 1995



REFERENCE COPY |  
Does Not |  
Circulate |

Bldg. 50 Library.

Copy 1

LBL-37729

## **DISCLAIMER**

This document was prepared as an account of work sponsored by the United States Government. While this document is believed to contain correct information, neither the United States Government nor any agency thereof, nor the Regents of the University of California, nor any of their employees, makes any warranty, express or implied, or assumes any legal responsibility for the accuracy, completeness, or usefulness of any information, apparatus, product, or process disclosed, or represents that its use would not infringe privately owned rights. Reference herein to any specific commercial product, process, or service by its trade name, trademark, manufacturer, or otherwise, does not necessarily constitute or imply its endorsement, recommendation, or favoring by the United States Government or any agency thereof, or the Regents of the University of California. The views and opinions of authors expressed herein do not necessarily state or reflect those of the United States Government or any agency thereof or the Regents of the University of California.

*Preliminary Analysis of Effects of  
Thermal Loading on Gas and  
Heat Flow within the Framework  
of the LBNL/USGS Site-Scale  
Model*

---

Y.S. Wu

G. Chen

G. Bodvarsson



**LAWRENCE BERKELEY NATIONAL LABORATORY**

This work was prepared under U.S. Department of Energy Contract No. DE-AC03-76SF00098, and DE-A108-78ET44802 administered by the Nevada Operations Office in cooperation with the U.S. Geological Survey, Denver.

---

# *TABLE OF CONTENTS*

---

|  |    |
|--|----|
| <b>SUMMARY</b> .....   | 1  |
| <b>1. INTRODUCTION</b> .....                                   | 2  |
| 1.1 Background .....   | 2  |
| 1.2 Previous Work .....  | 3  |
| 1.3 Treatment of Fracture and Matrix Flow .....                | 5  |
| 1.4 Objectives and Contents .....                              | 6  |
| <b>2. MODEL DESCRIPTION</b> .....                              | 8  |
| 2.1 Grid Design .....  | 8  |
| 2.2 Input Parameters .....                                     | 11 |
| 2.3 Boundary and Initial Conditions .....                      | 13 |
| <b>3. RESULTS AND ANALYSIS</b> .....                           | 16 |
| 3.1 Temperature and Saturation Changes at Repository .....     | 17 |
| 3.2 Vertical Temperature and Saturation Profiles .....         | 23 |
| 3.3 Effects of Thermal Loadings on Gas and Moisture Flow ..... | 27 |
| <b>4. CONCLUDING REMARKS</b> .....                             | 40 |
| <b>ACKNOWLEDGMENT</b> .....                                    | 42 |
| <b>REFERENCES</b> .....  | 42 |
| <b>FIGURES</b> .....   | 47 |

## SUMMARY

This report presents a modeling analysis of effects of thermal loading on gas and heat flow at a potential high-level nuclear waste repository of Yucca Mountain. The emphasis of this study is to investigate the hydro-thermal behavior of the unsaturated zone surrounding the repository under thermal loading using more realistic representations of the hydrogeologic system of the site.

The modeling study is based on the numerical simulations conducted using a two-dimensional vertical cross section of the west-east unsaturated zone, taken from the 3-D LBNL/USGS site-scale model. The cross-section studied is along N 233000, Nevada Coordinates, starting from E 16900 to the east with a total of length of about 4,400 m. Thermal sources are considered to be emplaced in two zones across Ghost Dance Fault along the lower middle portions of Topopah Spring with 6 m thickness, 1,200 m long for the west zone, and 800 m long for the east zone. The 2-D grid includes the variations of different hydrogeologic units along the cross-section, and explicit treatment of major faults.

The TOUGH2 code (Pruess, 1991) is employed in this study, and all the input parameters used for fluid and rock properties are from the site-scale model with rock thermal conductivities and heat capacity from RIB (DOE, 1993). Surface and bottom boundary conditions for the 2-D model are similar to those used in the site-scale model, i.e., constant pressures and temperatures specified. The initial condition of the cross-section corresponds to the steady-state condition, with zero net infiltration on the ground surface. For the repository, two thermal loading scenarios are considered: a) APD (Areal Power Density) = 57 kW/acre and b) APD = 114 kW/acre, respectively. The decay thermal source considered in the waste packages is from ten-year-old mixed waste.

The simulation results indicate that there is a strong influence of thermal loading on the gas and heat flow at the mountain. The averaged surface heat and gas flow has been increased by many orders of magnitude resulting from thermal loading over a period of tens of thousands of years. The major faults, Solitario Canyon fault and the Ghost Dance fault, serve as major pathways for heated gas and heat. These effects should be included in the future modeling studies.

# 1 INTRODUCTION

## 1.1 Background

---

The U. S. Department of Energy is performing detailed site characterization studies at Yucca Mountain to determine its suitability as a geological repository site for high level nuclear wastes. As part of these research efforts, a three-dimensional, site-scale unsaturated-zone model has been developed at Lawrence Berkeley National Laboratory (LBNL) in collaboration with the U. S. Geological Survey (USGS) (Wittwer et al., 1995). The primary objectives of developing the 3-D site-scale model are to predict the ambient hydrogeological conditions and the movement of moisture and gas within the unsaturated zone of the mountain. In addition, the model has the capability of modeling non-isothermal flow and transport phenomena at the mountain. Applications of such a site-scale model should include evaluation of effects of thermal loading on heated gas and heat flow through the mountain for long-term performance assessment of the repository.

Heat generated as a result of emplacing nuclear waste in a partially-saturated geological system will significantly affect the pre- and post-performance of the repository. Quantitative evaluation of thermo-hydrologic and thermal loading effects on the performance of the potential high-level nuclear waste repository at Yucca Mountain is essential in conducting site characterization studies and in designing the repository and engineering barrier system. Numerical modeling will play a crucial role in understanding the impact of thermal loading on various aspects of the overall waste disposal system, because it is impossible to observe and test thermo-hydrologic conditions over the time and space for the concerned waste site by laboratory or field studies alone. Performance assessment models based on numerical simulation of fluid and heat flow can include all important physical and chemical processes which affect repository and host rock behavior, and represent relevant thermo-hydrologic conditions at the potential repository site in full explicit details.

Emplacement of heat-generating high-level nuclear wastes at Yucca Mountain would create complex multiphase fluid flow and heat transfer processes. The physical mechanisms include conductive and convective heat transfer, phase change phenomena (vaporization and condensation), flow of liquid and gas phases under variably-saturated condition, diffusion and dispersion of vapor and gas, vapor sorption, and vapor-pressure lowering effects. The heterogeneity of complicated geological setting at Yucca Mountain, such as alternating layers of porous-fractured rocks, will significantly affect the processes of fluid and heat flow.

---

## 1.2 Previous Work

---

Numerical modeling approaches for simulating thermo-hydrologic and thermal loading processes are generally based on geothermal and petroleum reservoir simulation methodology using coupled multiphase fluid and heat flow formulations and finite difference or finite element schemes. A number of numerical repository performance models for evaluating the thermo-hydrologic loading effects of the Yucca Mountain site have been developed by several different groups (e.g. Pruess and Tsang, 1993 and 1994; Buscheck et al., 1991, 1992, 1994; and many others). Model conceptualizations focus mainly on large-scale average behavior or on local simplified domains of two-dimensional representations. In most cases the effective continuum approximation has to be used instead of explicit incorporation of fracture effects for treatment of matrix-fracture interactions, because of the intensity of computational requirement involved and uncertainties in site characterization of fracture and matrix properties.

Simulation techniques have been used to perform analyses of thermo-hydrologic conditions associated with high-level nuclear wastes since the early 1980's. Mondy et al. (1983) simulated fluid and heat flow using approximate two-dimensional representations of alternative emplacement geometries with and without ventilation of emplacement drifts. The host rock was modeled as an unfractured porous medium, and no allowance was made for vaporization or vapor transport (two-phase) effects.

Sensitivity studies on thermo-hydrological conditions near an infinite linear string of waste packages were reported by Pruess and Wang (1984). They modeled fluid and heat flow, including phase change effects in one-dimensional cylindrical geometry. They found that strong two-phase vapor-liquid counter-flow effects known as "heat pipe" (Ogniewicz and Tien, 1979; and Udell, 1985) occurred in some cases. The coupling with mechanical deformations of rocks has been investigated in field experiments by Zimmerman and coworkers (Zimmerman, 1983; Zimmerman et al., 1985; 1986). Studies of chemical composition and transport effects have been presented by a number of authors (e.g., Travis et al., 1984; Braithwaite and Nimick, 1984, Nielsen et. al., 1986; and Travis and Nuttall, 1987).

The early efforts in hydrologic performance assessment modeling were largely focused on either far-field infiltration under ambient conditions or hydrothermal flow in the near-field waste package environment. Numerical modeling studies have predicted the time-dependent temperature distribution within the emplacement boreholes or drifts and surrounding host rock for vari-



ous repository design, thermal loading conditions, and waste receipt and operating scenarios (Ryder, 1992; and Ruffner et al., 1993). However these models do not account for fluid phase change or heat transfer mechanisms other than thermal radiation or heat conduction.

Tsang and Pruess (1987) conducted repository-scale simulations with an emphasis on thermally driven natural convection. Nitao (1988) considered details of temperature, saturation, and gas-phase composition in the hydrothermally disturbed zone, using a model of a 3-km-diameter, disk-shaped repository, to examine the hydrothermal responses. Pruess, Wang and Tsang performed a comprehensive modeling study (1990a and 1990b) of simultaneous transport of heat, liquid water, vapor, and air in partially saturated fractured porous rock, using the TOUGH code (Pruess, 1987). They used a two-dimensional idealized model and included explicit consideration of fracture effects. The formation parameters they used were representative of the Yucca Mountain site of the nuclear waste repository. They investigated the range of parameters for which the effective continuum approximation in treating fracture and matrix interactions is valid. Their model included most of physical effects which were important in multiphase fluid and heat flow. They demonstrated the capability for modeling multiphase nonisothermal flow of water and air with phase change in a fractured medium and obtained certain insight into expected thermo-hydrological conditions near the waste packages.

A series of modeling studies of thermal loading impacts on thermo-hydrologic performance at Yucca Mountain have been performed by a group of researchers at the Lawrence Livermore National laboratory (LLNL) in the recent years. They have used the V-TOUGH code (Nitao, 1989), an LLNL-enhanced version of the TOUGH code, and the effective continuum approximation for treating fracture and matrix interactions. Many simulations and sensitivity studies have been conducted at LLNL in order to evaluate and predict the thermo-hydrologic conditions at the repository (Nitao, 1988; Nitao, 1990; Ramspott, 1991; Buscheck et al., 1991; Nitao, Buscheck and Chesnut, 1992; Buscheck and Nitao, 1992, 1993; Wilder, 1993; Buscheck, Nitao and Saterlie, 1994; and Buscheck and Nitao, 1994).

Some recently developed models (Pruess and Tsang, 1993; 1994) have provided more detailed investigations into strongly heat-driven flow processes at small scales to look at heterogeneity effects. They concluded through these studies that for a highly heterogeneous fractured-porous hydrogeologic system at Yucca Mountain, water movement within the unsaturated zone may be dominated by some highly localized phenomena, including "fast" channelized flow along preferential paths in fractures, and frequent local ponding. Current per-

formance assessment models focus on volume-averaged behavior and may not be able to represent such smaller-scale effects.

### *1.3 Treatment of Fracture and Matrix Flow*

---

The key issue for simulating fluid and heat flow in fractured porous media, the welded units of the Yucca Mountain site, is to evaluate fracture and matrix interactions under multi-phase, non-isothermal conditions. There are several methods for treating fracture and porous matrix interactions using a numerical model. The available methods include: (1) explicit discrete fracture and matrix interaction; (2) effective continuum approach; (3) double porosity method; (4) dual-permeability method; and (5) multiple interacting continua (MINC) method (Pruess and Narasimhan, 1985). When applied to simulating moisture flow and heat transfer in the mountain, all these approaches require knowledge of fracture and matrix properties and their spatial distribution for use. These site-specific fracture/matrix parameters, however, are not well defined at present for the Yucca Mountain site. Currently only the effective continuum approach has found wide applications because of its simplicity in terms of data requirements and computational intensity.

As implemented in the site-scale model (Wittwer et al., 1994; 1995) with the TOUGH2 code, the effective continuum approach can accommodate two-phase flow in a fracture/matrix system. It should be noted that this method is based on an assumption that local thermodynamic equilibrium exists between the fracture and matrix system (Pruess et al., 1990b). When applicable it provides a substantial simplification in the description of fluid and heat flow in fractured porous media. Favorable conditions for this method are present when rock matrix blocks are relatively small and permeable and fracture network is relatively uniformly distributed. However, the effective continuum approximation may break down under certain unfavorable conditions, such as for very tight, large and low permeable rock matrix under rapid transient perturbations, since it may take a long time to reach equilibrium under such conditions.

At Yucca Mountain, the net infiltration rate into the unsaturated zone has been estimated to be low, of the order of 1 mm/yr. The rate of water movement through the mountain is expected to be small in most parts of the mountain. Therefore, the local hydraulic equilibrium between porous rock matrix and fractures may be a reasonable approximation. As a result, the effective continuum approach may provide reasonable simulation results for predicting the moisture movement and the ambient hydrogeologic conditions. The continuum method will be particularly suitable for a situation when a long-term, averaged, or

steady-state solution is to be sought. As concluded by Pruess et al. (1990b), the effective continuum approximation will be applicable when "sufficiently" large space and time scales are considered. Both time and space discretizations in the three-dimensional site-scale unsaturated-zone model are relatively coarse, and the application of the continuum approach may be justified for time and space scales of interest to the site-scale modeling studies.

#### *1.4 Objectives and Contents*

Current thermal loading assessment studies are mostly based on simple geometric models of 1-D and 2-D (R-Z), or 2-D (X-Z) cross-sectional grids to represent the repository system. In these models the different hydrogeologic units and heterogeneous formations at Yucca Mountain are approximated using simplified horizontal layers with uniform thickness for each sublayer. Such models can provide insight into the average thermal and hydrologic behavior. They may also be useful for performing certain sensitivity studies and for looking at mechanisms governing heat transfer and fluid movement associated with the thermal loading. However, certain important issues, such as effects of 3-D geological structures with dipping layerings and major faults on thermo-hydraulic conditions, have not been addressed.

The Yucca Mountain site, according to current conceptualizations, is a highly heterogeneous fractured-porous geological system, consisting of thick layers (up to several hundred meters) of alternating welded and nonwelded units with large contrast in degrees of fracturing and rock matrix permeability and porosity. The potential repository horizon is at the lower middle portions of a highly-fractured, Topopah Spring, welded unit. Many different-type faults have been observed to exist within and near the repository areas, and the effects of these faults on the two-phase fluid and heat flow under the thermo-hydrologic conditions are not well understood. Even though a substantial amount of site characterization studies have been conducted so far to determine the properties and variabilities of heterogeneous layers, fracture network and matrix rock characteristics, and water retention functions, many of the important hydrologic parameters are not well defined at present.

In this work, we investigate the possibility of applying the site-scale model to evaluating the effects of repository thermal loading on gas and heat flow. The site-scale model provides a much more realistic representation of the hydrogeologic system for the unsaturated zone at Yucca Mountain. The 3-D model geometry and grid have been defined (1) to represent the variations of hydrogeological units between the ground surface and the water table; (2) to be able

to reproduce the effect of abrupt changes in hydrogeological parameters at the boundaries between hydrogeological units; and (3) to include the influence of major faults.

This report presents numerical test results based on our recent modeling studies on thermal loading analysis using a 2-D submodel, extracted from the 3-D site-scale model grid. The objective of this study is to look at the hydro-thermal behavior at the unsaturated zone surrounding the repository under thermal loading conditions when a more realistic representation of the hydrogeologic system is used.

The modeling study of this report is based on the numerical simulations conducted using a two-dimensional vertical cross section of the west-east unsaturated zone, taken from the 3-D LBNL/USGS site-scale model. The cross-section is along N 233000, Nevada Coordinates, starting from E 16900 to the east with a total length of about 4,400 m. Thermal sources are considered in two zones across Ghost Dance fault along the lower middle portions of Topopah Spring with 6 m thickness. The "upper" block is 1200 m long for the west zone, and the "lower" is 800 m long for the east zone. The 2-D grid includes the variations of different hydrogeologic units along the cross-section, and explicit treatment of major faults.

The TOUGH2 code is used in this study, and all the parameters used for fluid and rock properties are from the site-scale model, and the rock thermal conductivities and heat capacity are from RIB (DOE, 1993). Surface and bottom boundary conditions are similar to those for the site-scale model, i.e., constant pressures and temperatures specified. The initial condition of the system corresponds to the steady-state, ambient condition, with zero net infiltration. At the repository, two thermal loading scenarios are considered: a) APD = 57 kW/acre and b) APD = 114 kW/acre. The decay thermal source considered is ten-year-old mixed waste (Pruess and Tsang, 1994).

The simulations indicate that there is a strong influence of thermal loading on the gas and heat flow in the mountain. The averaged surface heat and gas flow is predicted to be increased by many orders of magnitude as a result of thermal loading, and the Solitario Canyon fault and the Ghost Dance fault both serve as major pathways for gas and heat. The modeling results show that it is necessary for future modeling investigations to use more realistic representations of the unsaturated zone and include the effects of the major faults.

## 2. MODEL DESCRIPTION

### 2.1 Grid Design

---

In order to reasonably represent the repository thermal loading system using a 2-D model, it should be taken into account that there exist different hydrogeologic, welded and nonwelded, units, layering and dipping of the formation, and the major faults at the mountain. The grid design also needs to consider the recommended layout plan of the repository drifts for a more realistic modeling study.

In this study, a 2-D vertical cross-sectional grid is designed according to the repository layout option X. As a result of the development and evaluation of the repository layout concepts of the Yucca Mountain project, two final options have been proposed (M&O, 1995), X and Y. The first layout option X has been a "preferred" concept, or base case, and will be used as the primary basis for repository advanced conceptual design. The option Y layout is designated as an alternate concept. According to the option X (M&O, 1995), the repository will be designed to consist of two emplacement blocks, upper and lower, containing the flat-lying emplacement drifts within the TSw unit. The "upper" emplacement block is located to the west of the Ghost Dance fault, and the "lower" block is situated at an elevation that is approximately 70 meters lower than the "upper" emplacement block to the east of the Ghost Dance fault. The diameter of waste emplacement drifts for either layout options could vary between 5.0 to 6.5 meters.

A 2-D vertical cross-sectional grid adopted for this study is designed to cross both the emplacement blocks from west to east. Shown in Figure 1 is a plan view of the cross-section (A-A') location, the repository blocks, major faults, and the associated site-scale model domain. The 2-D cross-section starts at the Nevada Coordinates, E 16900, to the east along the N 233000 coordinates with a total length of 4,400 m. The repository drifts in both the west "upper" block and the east "lower" one are represented in the grid as horizontal sublayers with thickness of 6 m. The western repository block is 1,200 m long with an elevation of 1070, and the eastern one is 800 m long with an elevation of 1,000 m.

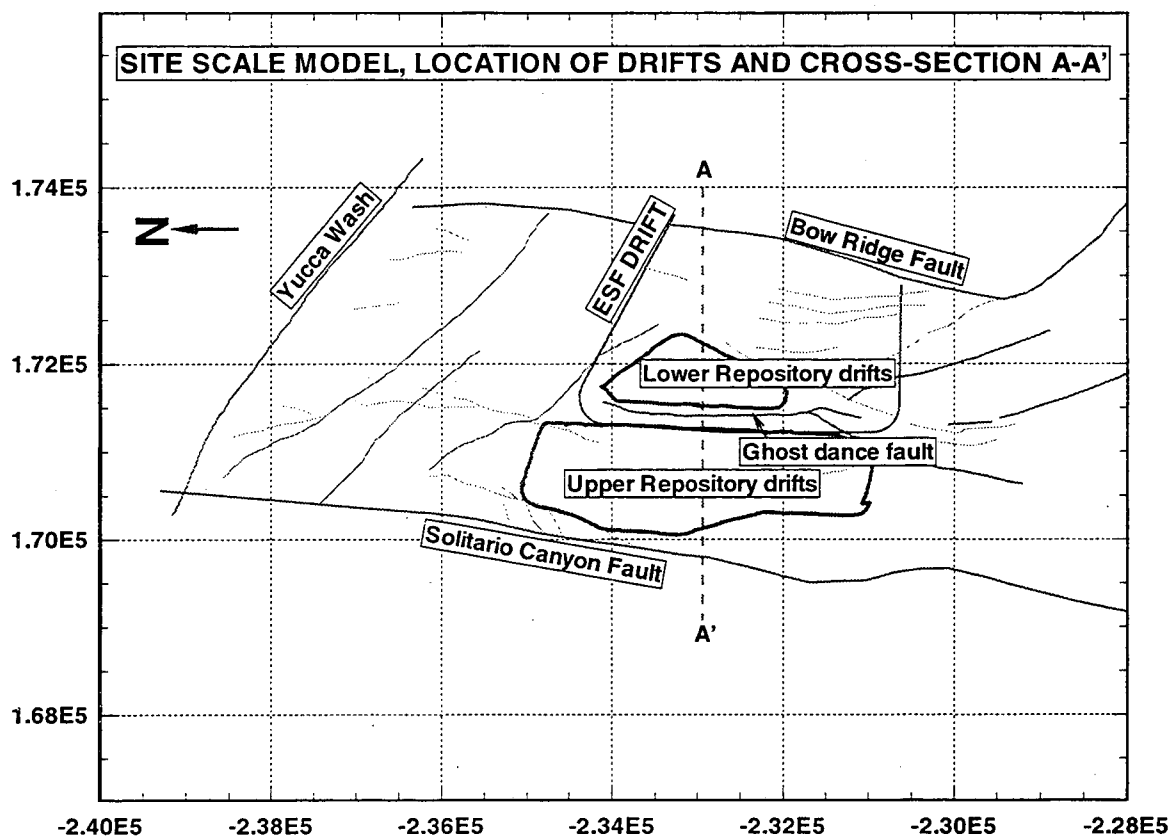


Figure 1.

A plan view of the potential repository at Yucca Mountain, showing the two waste emplacement blocks, major faults, the cross-section, and the site-scale model domain.

The 2-D cross-sectional grid used in this study, shown in Figure 2, consists of 31 subgrid layers and 74 rock columns, with a total of 2,425 elements. Much finer meshes, compared with the 3-D grid of the site-scale model, are used for both the vertical and horizontal dimensions in order to obtain better numerical resolutions within the domain near the repository. This is necessary because strong transient multiphase flow, rapid conduction and convection heat transfer, associated with boiling and large latent heat effects, will take place at the repository under thermal loading conditions. Use of large mesh blocks in the model at the repository may under-estimate the highest temperature and associated fluid movement near the repository for the same decayed heat source, since the model's predictions are averages over the mesh blocks.

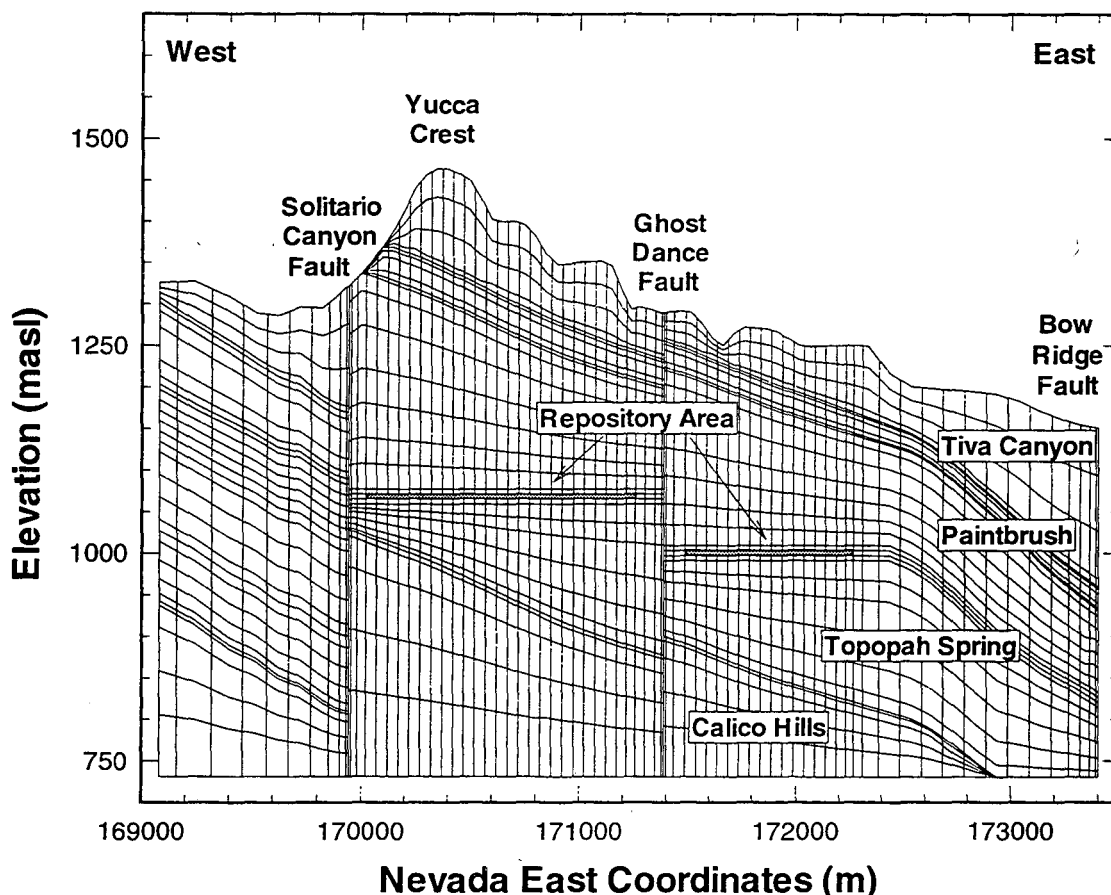


Figure 2.

Grid of the 2-D west-east cross-section along the Nevada Coordinates N 233000.

It should be mentioned that the grid lines shown in Figure 2 are curving or dipping in the horizontal direction. This is the result of computer smoothing with the plot. The actual elemental blocks are all rectangular with flat horizontal boundaries. The 2-D grid was generated using a 3-D grid generator, developed to fulfill the integral finite difference method of the TOUGH2 code (Wittwer et al., 1995). The grid generator ensures all the interface connections in the plane are perpendicular to the flow directions. The scheme used for generating fault gridblocks with offsets within the 2-D grid was discussed by Wittwer et al. (1995), in which a fault is treated as a porous media zone with appropriate connections to adjacent gridblocks or offsets.

The hydrogeologic unit division considered in the 2-D model follows the framework of the 3-D site-scale model, and the unsaturated zone is divided into

four major units, Tiva Canyon (TCw), Paintbrush (PTn), Topopah Spring (TSw), and Calico Hills (Chn), from top to water table. Each of the units is further subdivided into a number of sub-grid layers. The major faults included are the Solitario Canyon fault and Ghost Dance fault. The Bow Ridge fault is used as the eastern boundary. The faults are represented in the model by vertical rock columns with thickness of 20 m, vertically crossing the entire unsaturated zone, specified with a porous medium property. The original western boundary of the site-scale model coincides with the Solitario Canyon Fault, and the eastern boundary is at the Bow Ridge Fault. In this study, we keep the eastern boundary at the same location, but extend the western model boundary 1,000 m further west into the Solitario Canyon to reduce the possible boundary effects associated with the Solitario Canyon fault. This extension of the model boundary is necessary because, as shown in Figure 1, the Solitario Canyon fault is very close to the referred repository location, the "upper" western block.

## 2.2 Input Parameters

The 3-D site-scale unsaturated-zone model of Yucca Mountain, which is under continuous development and enhancement at LBNL (Wittwer et al., 1995), provides a complete set of parameters for simulating the fluid and heat flow through the unsaturated zone of the mountain. In the present 2-D study all the model input data, properties of fluids and rocks, hydrogeological units and divisions, and soil characteristic curves are kept to be identical to those used in the site-scale model. We also use the same convention, i.e., specifying the parameters layer-wise. However, a much finer grid is designed for the current thermal loading analysis than the 3-D site-scale model grid, therefore certain adjustments in converting the soil properties from large to small blocks are needed. Table 1 lists the rock matrix and the fault properties as used in this simulation study

| Hydrogeological unit | Model sublayers | Porosity <sup>(a)</sup> | Permeability <sup>(a)</sup> (m <sup>2</sup> ) | v. G. $\alpha^{(a)}$ (Pa <sup>-1</sup> ) | v. G. m <sup>(a)</sup> | Thermal conductivity <sup>(b)</sup> (W/m <sup>o</sup> C) | Grain density <sup>(c)</sup> (kg/m <sup>3</sup> ) | Specific heat <sup>(b)</sup> (J/kg <sup>o</sup> C) |
|----------------------|-----------------|-------------------------|---|--|------------------------|--|---|--|
| TCw                  | 1.1             | 0.17                    | 1E-18   | 6.7E-7                                   | 0.25                   | 1.73   | 2480  | 935.82   |
|                      | 1.2             | 0.17                    | 1E-18   | 6.7E-7                                   | 0.25                   | 1.73   | 2480  | 935.82   |
|                      | 1.3             | 0.17                    | 2E-18   | 6.7E-7                                   | 0.25                   | 1.73   | 2480  | 935.82   |
|                      | 1.4             | 0.17                    | 2E-18   | 6.7E-7                                   | 0.25                   | 1.73   | 2480  | 935.82   |
|                      | 1.5             | 0.06                    | 1E-18   | 6.7E-7                                   | 0.25                   | 1.73   | 2480  | 826.31   |



| Table 1. Rock matrix properties for the 31 sublayers derived from the 17 sublayers of the SSM. |                 |                         |   |  |                        |  |   |  |
|--|-----------------|-------------------------|---|--|------------------------|--|---|--|
| Hydrogeological unit   | Model sublayers | Porosity <sup>(a)</sup> | Permeability <sup>(a)</sup> (m <sup>2</sup> ) | v. G. $\alpha^{(a)}$ (Pa <sup>-1</sup> ) | v. G. m <sup>(a)</sup> | Thermal conductivity <sup>(b)</sup> (W/m <sup>0</sup> C) | Grain density <sup>(c)</sup> (kg/m <sup>3</sup> ) | Specific heat <sup>(b)</sup> (J/kg <sup>0</sup> C) |
| PTn  | 2.1             | 0.33                    | 5E-14   | 1.67E-5                                  | 0.167                  | 0.85   | 2300  | 1375.4   |
|  | 2.2             | 0.37                    | 5E-14   | 6.0E-5                                   | 0.163                  | 0.85   | 2300  | 1460.5   |
|  | 2.3             | 0.37                    | 5E-14   | 6.0E-5                                   | 0.163                  | 0.85   | 2300  | 1460.5   |
| PTn (cont.)  | 2.4             | 0.37                    | 1E-13   | 6.0E-5                                   | 0.163                  | 0.85   | 2300  | 1460.5   |
|  | 2.5             | 0.37                    | 1E-13   | 4.33E-5                                  | 0.142                  | 0.85   | 2300  | 1353.2   |
| TSw  | 3.1             | 0.06                    | 1E-18   | 6.7E-7                                   | 0.29                   | 1.70   | 2480  | 848.28   |
|  | 3.2             | 0.15                    | 4E-16   | 1.25E-6                                  | 0.18                   | 1.70   | 2480  | 938.28   |
|  | 3.3             | 0.15                    | 4E-16   | 1.25E-6                                  | 0.18                   | 1.70   | 2480  | 938.28   |
|  | 3.4             | 0.13                    | 4E-18   | 2.0E-6                                   | 0.22                   | 1.60   | 2480  | 916.71   |
|  | 3.5             | 0.13                    | 4E-18   | 2.0E-6                                   | 0.22                   | 1.60   | 2480  | 916.71   |
|  | 3.6             | 0.13                    | 4E-18   | 2.0E-6                                   | 0.22                   | 1.60   | 2480  | 916.71   |
|  | 3.7             | 0.13                    | 4E-18   | 2.0E-6                                   | 0.22                   | 1.60   | 2480  | 916.71   |
|  | 4.1             | 0.13                    | 4E-18   | 2.0E-6                                   | 0.22                   | 1.60   | 2480  | 916.71   |
|  | 4.2             | 0.13                    | 4E-18   | 2.0E-6                                   | 0.22                   | 1.60   | 2480  | 916.71   |
|  | 4.3             | 0.14                    | 5E-18   | 2.0E-6                                   | 0.25                   | 2.10   | 2480  | 952.93   |
|  | 5.1             | 0.14                    | 5E-18   | 1.33E-6                                  | 0.25                   | 2.10   | 2480  | 952.93   |
|  | 5.2             | 0.14                    | 5E-18   | 1.33E-6                                  | 0.25                   | 2.10   | 2480  | 952.93   |
|  | 5.3             | 0.14                    | 5E-18   | 1.33E-6                                  | 0.25                   | 2.10   | 2480  | 952.93   |
|  | 5.4             | 0.14                    | 5E-18   | 6.7E-7                                   | 0.25                   | 2.10   | 2480  | 931.27   |
|  | 5.5             | 0.12                    | 5E-18   | 6.7E-7                                   | 0.25                   | 2.10   | 2480  | 931.27   |
| 5.6  | 0.12            | 1E-18                   | 2.0E-6  | 0.29                                     | 1.28                   | 2480   | 782.81  |  |
| CHn  | 7.1             | 0.13                    | 2E-13   | 2.0E-6                                   | 0.13                   | 1.20   | 2300  | 1634.5   |
|  | 7.2             | 0.13                    | 3E-13   | 2.0E-6                                   | 0.12                   | 1.20   | 2300  | 1451.1   |
|  | 7.3             | 0.13                    | 3E-13   | 2.0E-6                                   | 0.12                   | 1.28   | 2300  | 1855.4   |
|  | 7.4             | 0.13                    | 1E-15   | 2.0E-6                                   | 0.19                   | 1.56   | 2300  | 1509.1   |
|  | 7.5             | 0.13                    | 1E-15   | 1.0E-6                                   | 0.19                   | 1.56   | 2300  | 1425.3   |
| Solitario Canyon   | Fault           | 0.30                    | 1E-13   | 1.93E-6                                  | 0.80                   | 1.50   | 2390  | 1195.5   |
| Ghost Dance  | Fault           | 0.30                    | 1E-11   | 6.11E-6                                  | 0.50                   | 1.50   | 2390  | 1195.5   |

(a) Wittwer et al., 1994 (b) DOE (RIB), 1993 (c) Pruess and Tsang, 1994

The fracture system in the two welded units, Tiva Canyon, and Topopah Spring, is treated using the effective continuum approach (Pruess et al., 1990b; and Pruess and Tsang, 1994) with a constant value of fracture permeability of  $10^{-11}$  m<sup>2</sup> and a porosity of 0.1%, the same as used for the site-scale model. The properties for the Ghost Dance fault are kept to be the same as those (Table 1) in the site-scale model. For the Solitario Canyon fault, the selected parameters are provided in Table 1.

### 2.3 *Boundary and Initial Conditions*

---

The land surface along the west-east cross-section of Yucca Mountain is used as the top model boundary. The actual top boundary is subject to the variations of humidity, temperature, and pressure in the atmosphere daily and seasonally. The interactions of the top soil and the atmospheric conditions are, however, approximated in this model using land surface boundary conditions of constant air pressure for each rock column, a constant temperature of 13 °C, and zero net water infiltration. This type of treatment of the top boundary can give reasonable results for simulating moisture, gas and heat flow in terms of long-term and averaged model predictions.

Use of constant or averaged temperatures on the surface is a reasonable approximation to simulate the natural geothermal gradient or the natural and undisturbed system. The atmospheric and soil surface temperature and its variations have little effect on the geothermal conditions of the formation more than 20 m deep from the surface. However, the surface temperatures may increase under the thermal loading conditions at the repository, depending on thermal loading scenarios, and the design depth of the repository among others. The possible effects of the increased soil surface temperature on the predicted results are not considered in the present study.

The water table has been used as the bottom boundary for this study, as in most of the unsaturated-zone models. As incorporated in the current 3-D site scale model, the water table is represented as a relatively flat, stable surface at an approximate elevation of 730 m. Under thermal loading conditions, however, the temperature at the water table will also increase and these temperature variations at the water table need to be considered in future modeling studies for long-term performance assessment of the repository. The bottom water table condition in this work is described with a constant air pressure of 0.927 bar and a constant temperature of 32 °C.

The top surface air pressure values for different rock columns and the initial boundary condition in the cross-section are generated by running the TOUGH2 code to steady-state, subject to the model conditions discussed above. The initial water saturation distribution is shown in Figure 3, and the initial temperature distribution is shown Figure 4. As shown in Figure 3, the saturation is about 0.6 - 0.7 at the repository horizons, which is close to the results of Buscheck and Nitao (1993b).

In the initialization and the following thermal loading simulations, the module of EOS3 of the TOUGH2 code has been used, and the vapor pressure lowering effects have been ignored. The vapor-air diffusion process has been included, but no "enhancement" of vapor diffusion is considered in this study. The "enhanced" vapor diffusion nature may be important to the flow and transport processes at Yucca Mountain, however, it is currently subject to many uncertainties due to the lack of field or laboratory data from the site.

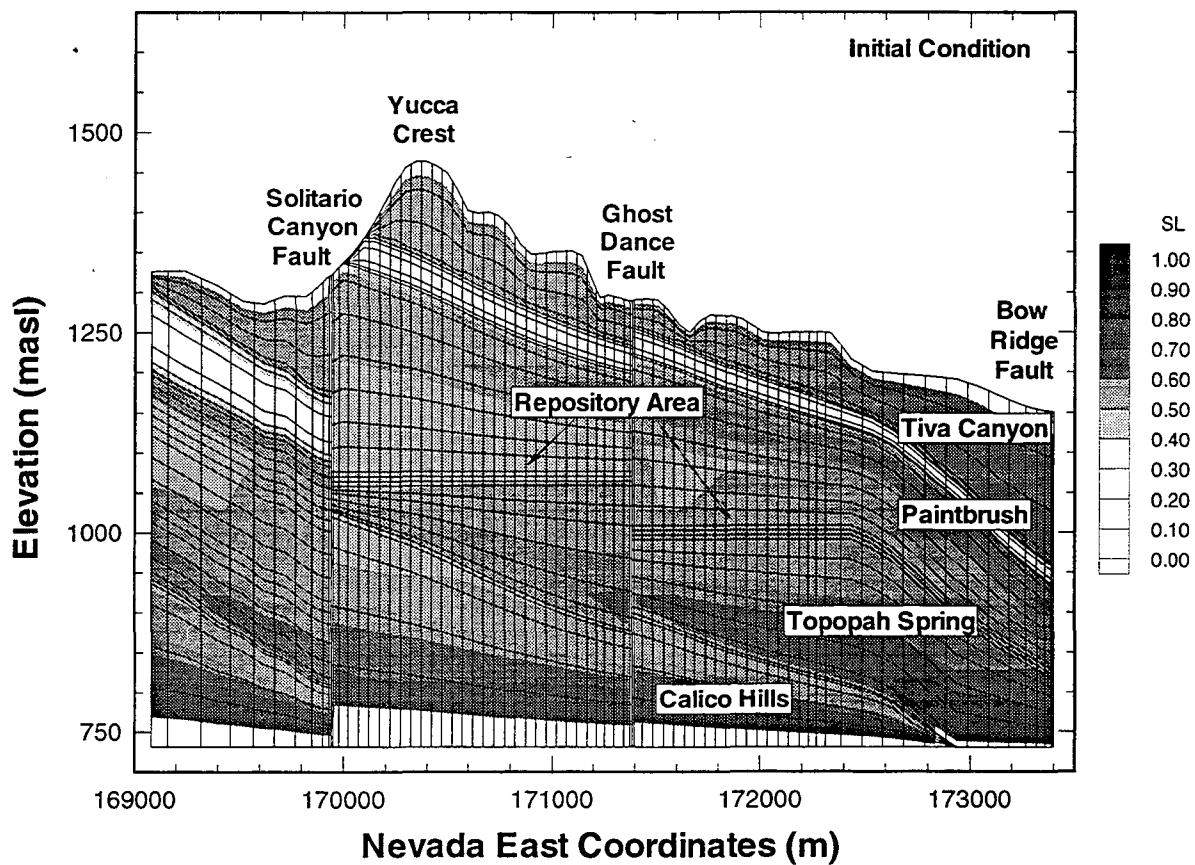


Figure 3.  
The initial distribution of liquid saturation in the cross-section.

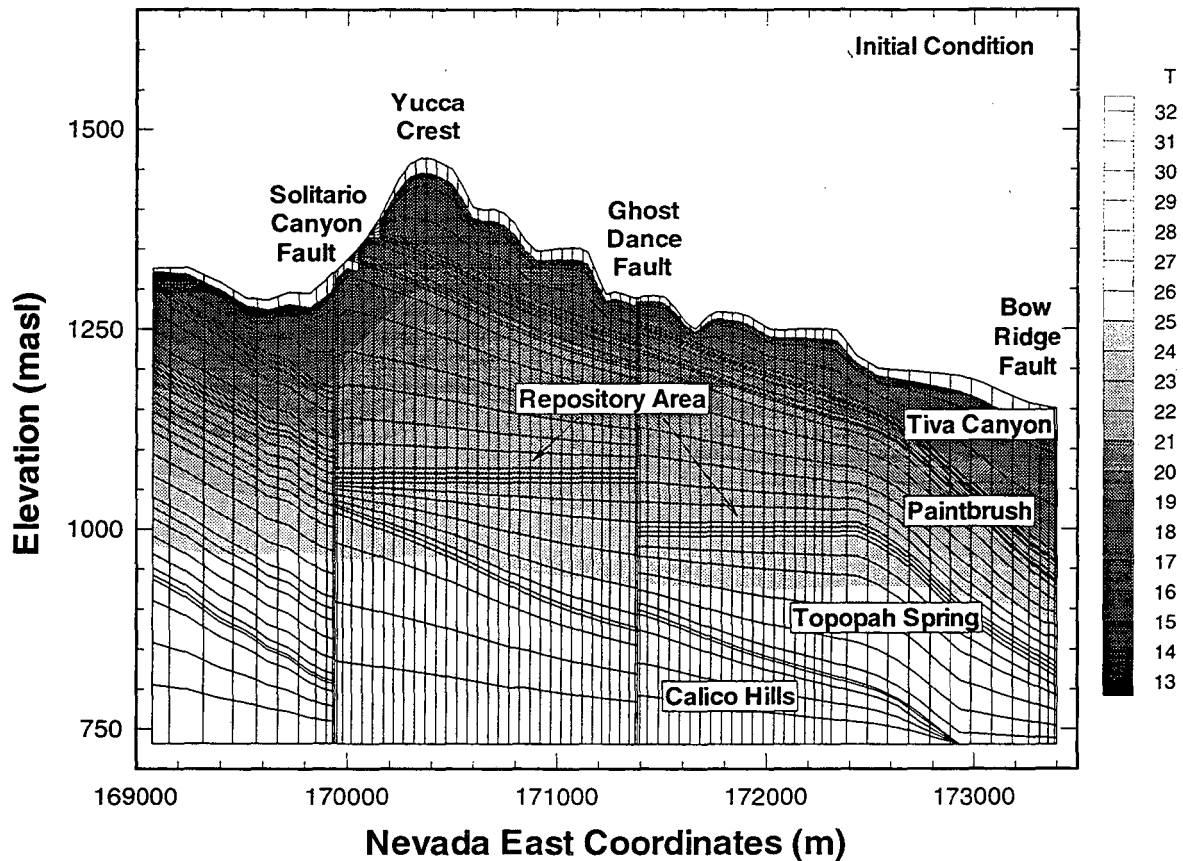


Figure 4.  
The initial distribution of temperature in the cross-section.

### 3. RESULTS AND ANALYSIS

Emplacement of high-level nuclear waste in the unsaturated fractured and matrix tuffs with highly heterogeneous materials at Yucca Mountain will be subject to many physical processes under thermo-hydrologic conditions. There will exist strong two-phase flow effects in the system. As heat is released from the waste unit and transferred to the surrounding host rock, temperatures near the waste packages will approach or exceed the boiling point of water (appxi-

mately 96 °C at ambient pressure). Vaporization of formation water will then take place, with associated increases in vapor partial pressure and overall gas phase pressure. This will result in forced convection of the gas phase with redistribution of water component accompanied by large latent heat effects. The phase transformation and gas phase flow will perturb the in-situ fluid saturation distribution in both fractures and matrix, thereby setting up capillary pressure gradients and liquid phase flow.

The thermo-hydrologic behavior of the mountain depends on the thermal loading among other factors. Thermal loadings are expressed in terms of Areal Mass Loading (AML) (MTU/acre), or Areal Power Density (APD) (kW/acre) to account for radioactive heat of decay. AML or APD values with waste type in a repository of given design will determine the total thermal energy introduced into and subsequent heat released from the system. The higher AML or APD, the more energy input, and the stronger thermo-hydrologic effects will be expected. There are two thermal loading scenarios considered in this study, one with APD = 57 kW/acre and the other with APD = 114 kW/acre, and they will be referred to as the lower and higher thermal loading scenarios, respectively, in the following. The decay thermal source is ten-year-old mixed waste (Pruess and Tsang, 1994). It should be mentioned that for both loading scenarios, the same repository emplacement blocks are used in the simulations. Since this is a 2-D simulation analysis, the higher loading scenario corresponds to a much smaller repository area for each emplacement block, i.e., the South-North extension of the repository reduces to only the half of the layout area for the lower thermal loading condition.

### *3.1 Temperature and Saturation Changes at Repository*

Figures 5 and 6 show the temperature and saturation variations with time up to 100,000 years for the two thermal loading scenarios, respectively, at a location within the central portion of the eastern emplacement block. The simulation results, as shown Figures 5 and 6, indicate that the highest temperature reached at the repository location is 162 °C for the high APD and 103 °C for the low APD. Boiling conditions for water are reached in both cases. The boiling period for the higher loading starts at 5 years and lasts until 2,700 years. For the lower loading scenario of APD = 57 kW/acre, as shown in Figure 6, the boiling period is much shorter, and lasts from 20 to 500 years. The saturation changes at the repository of Figures 5 and 6 reveal that complete dryout zones are developed at the repository for both thermal loading options. The dryout period with zero liq-

uid aid saturation lasts from 15 to 19,000 years for APD = 114 kW/acre, but lasts only from 60 to 1,500 years under the lower thermal loading. However, the complete dryout created here may not fully reflect the actual physical conditions on a small-scale at the repository since effects of residual water saturations and the vapor-pressure lowering effects are ignored in the simulations. The simulated dryout phenomena also correspond to the averaged behavior of the grid, which is relatively large (6x50m) for including small-scale local fracture and matrix heterogeneities. Some recent studies (Pruess and Antunez, 1995) indicated that liquid phase may exist in heterogeneous fractures even when temperature is much higher than the local boiling point, due to the effects of the vapor pressure lowering and local heterogeneities.

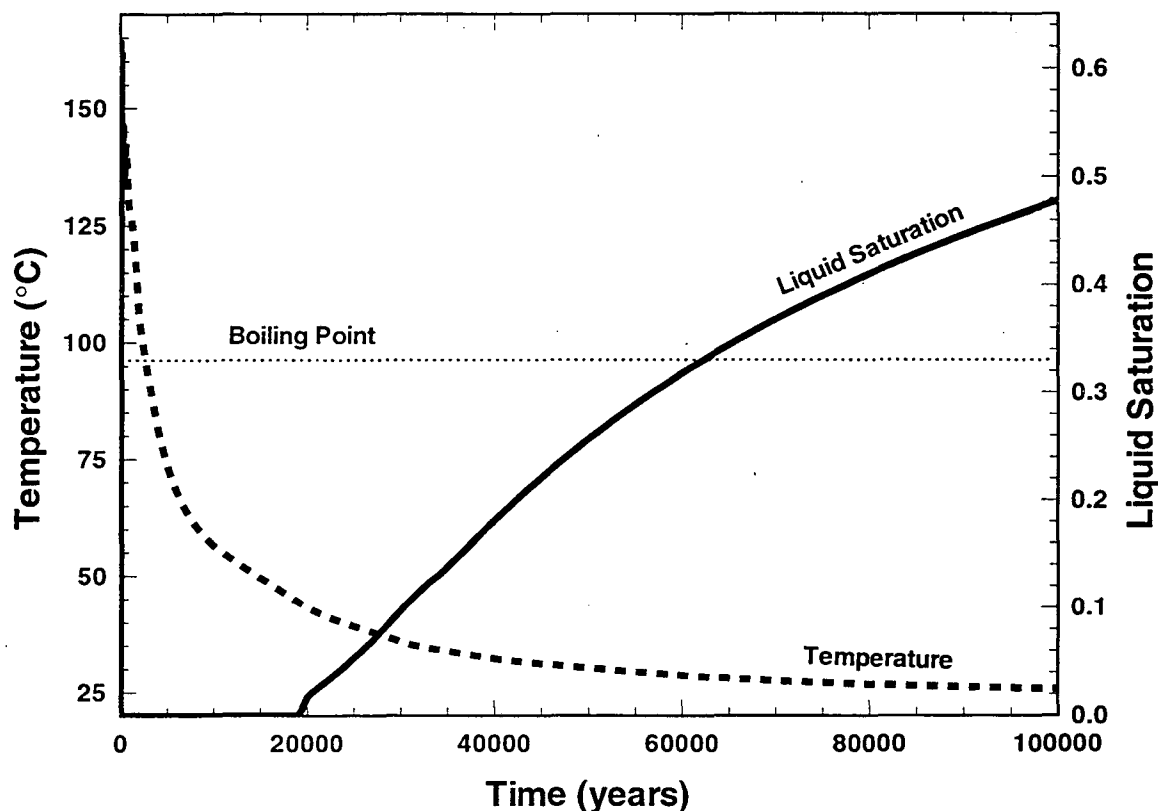


Figure 5.

Variations in temperature and saturation at the center of the eastern emplacement block for APD = 114 kW/acre.

Initially, the saturation at this location of the repository is about 0.61, then the saturation decreases to or near zero during the boiling period, and later it increases gradually. However, the rewetting process for the dryout zones is slow following the boiling period. As shown in Figure 5, the saturation still has not recovered to its original value even at 100,000 years for the higher loading condition. For the lower loading, the saturation returns almost to the original level.



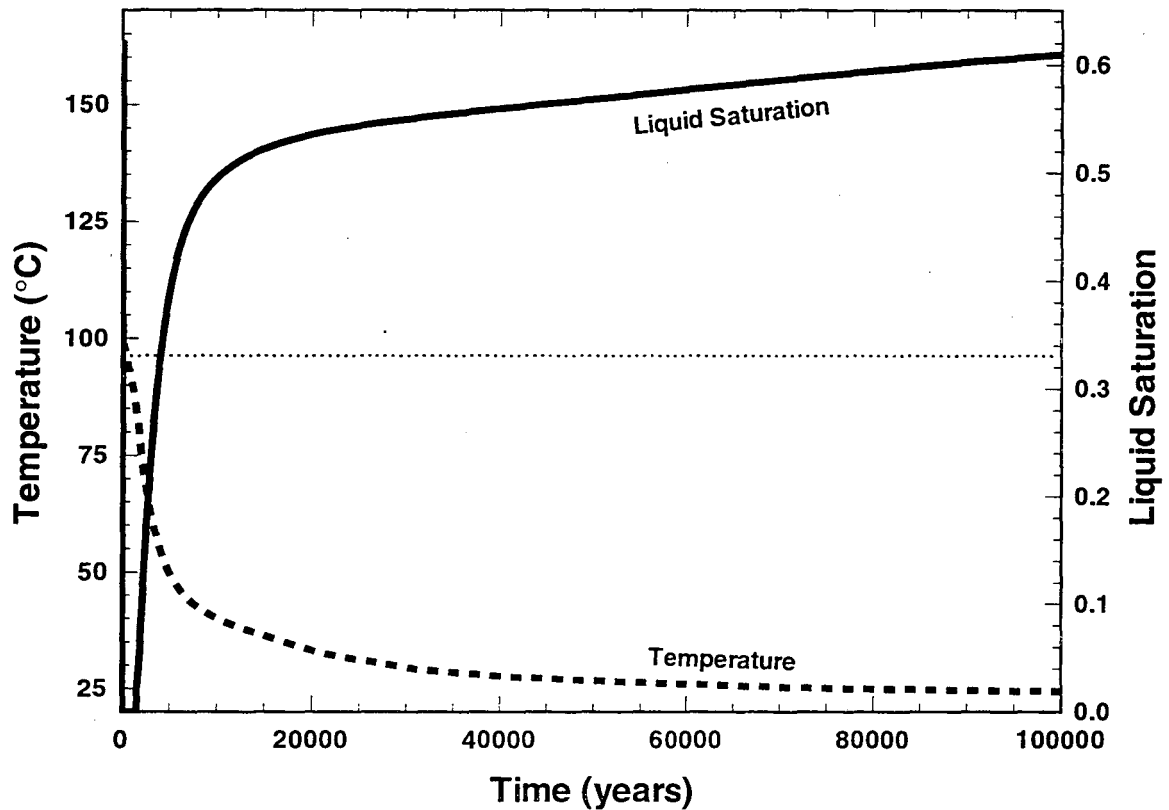


Figure 6.

Variations in temperature and saturation at the center of the eastern emplacement block for APD = 57 kW/acre.

Figures 7 and 8 present the temperature variations near the ground surface, immediately above the repository. As shown in these figures, the temperature rises after 200 - 400 years after the disposal and reaches its peak values in about 600 to 800 years. After 1,000 years, the temperature decreases steadily.

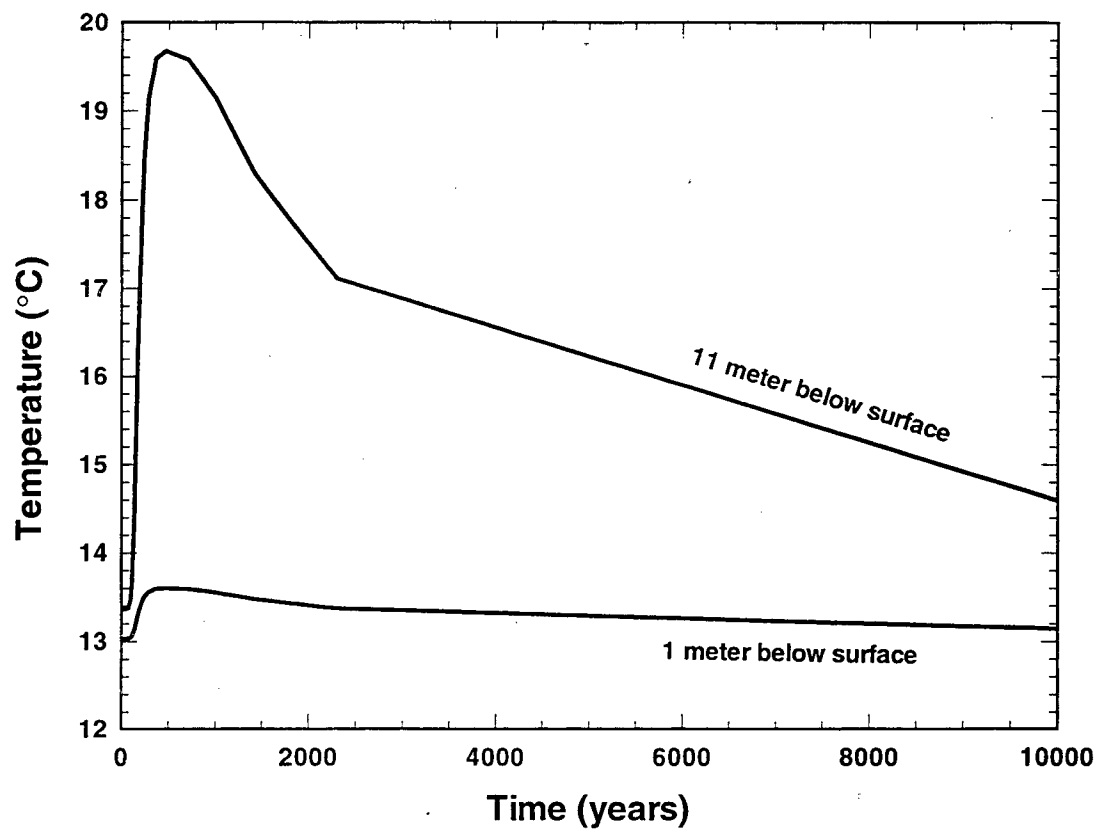


Figure 7.

Temperature increases near the ground surface above the repository for APD = 114 kW/acre.

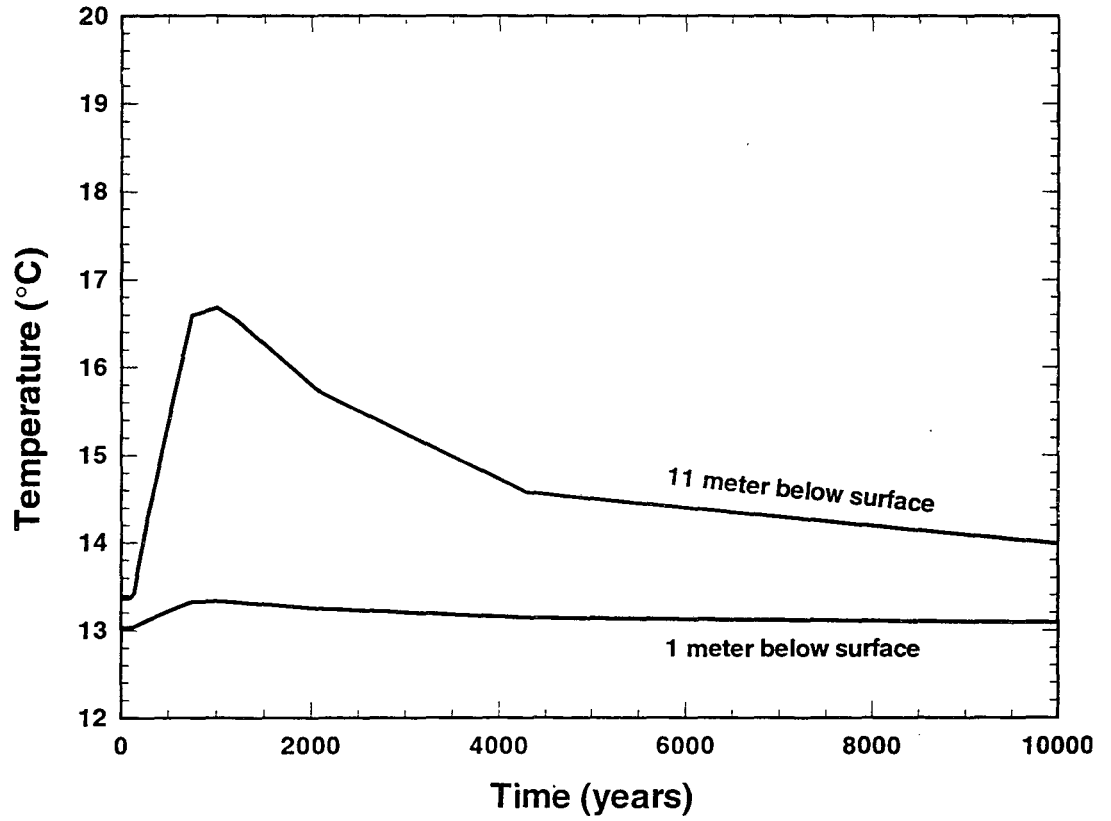


Figure 8.

Temperature increases near the ground surface above the repository for APD = 57 kW/acre.

---

### 3.2 *Vertical Temperature and Saturation Profiles*

---

Vertical temperature profiles, taken at the center of the eastern repository block, are shown in Figures 9 and 10. It can be seen that the temperature maximum is always at the repository horizon. For the higher loading scenario, the temperature at the waste horizon increases to the maximum of about 160 °C in 50 years, and then begins to decline. It is interesting to note that "heat pipe" conditions have been created in the zone at and above the repository horizon, as shown in Figures 9 and 10. The heat pipe phenomena are indicated by the vertical temperature profiles at times between 50 and 1,000 years. The temperature values at which heat pipe conditions occur correspond to the boiling point under ambient condition of moisture and atmospheric pressure. For the lower thermal loading, very weak "heat pipe" behavior can be seen in Figure 10 for the times between 100 and 270 years.

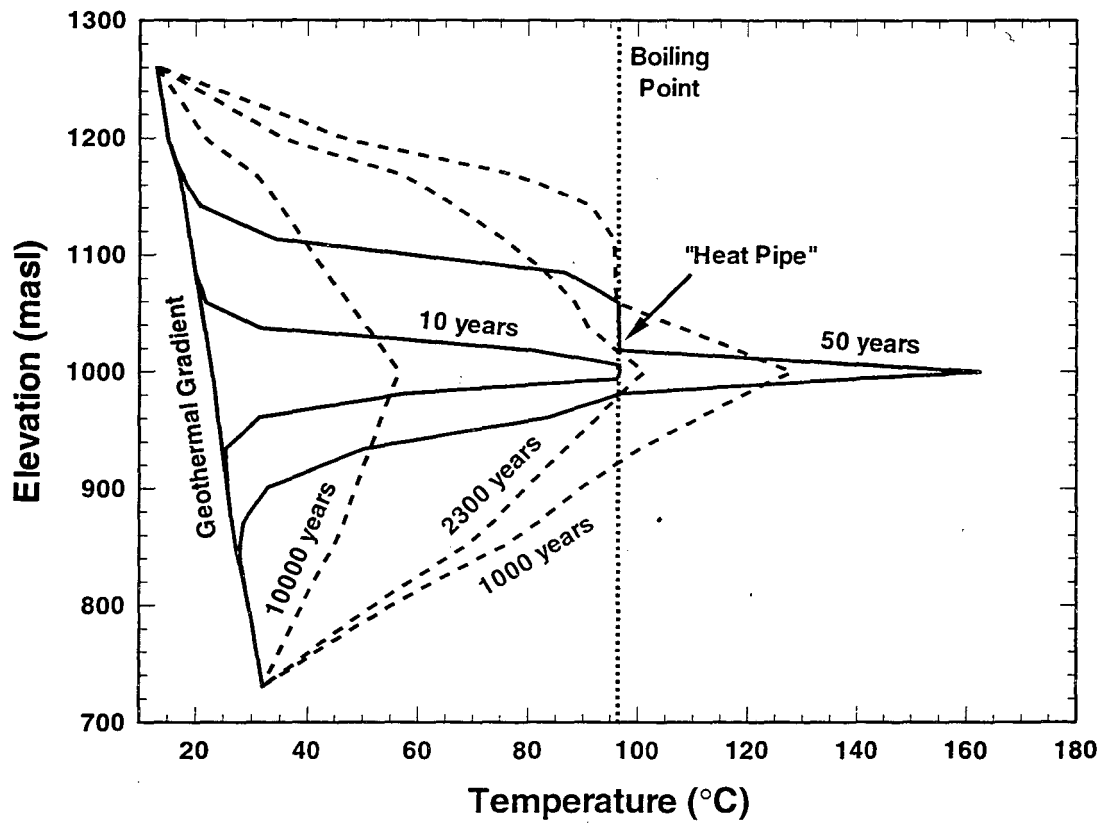


Figure 9.

Vertical temperature profiles along the repository centerline of the eastern emplacement block for APD = 114 kW/acre.

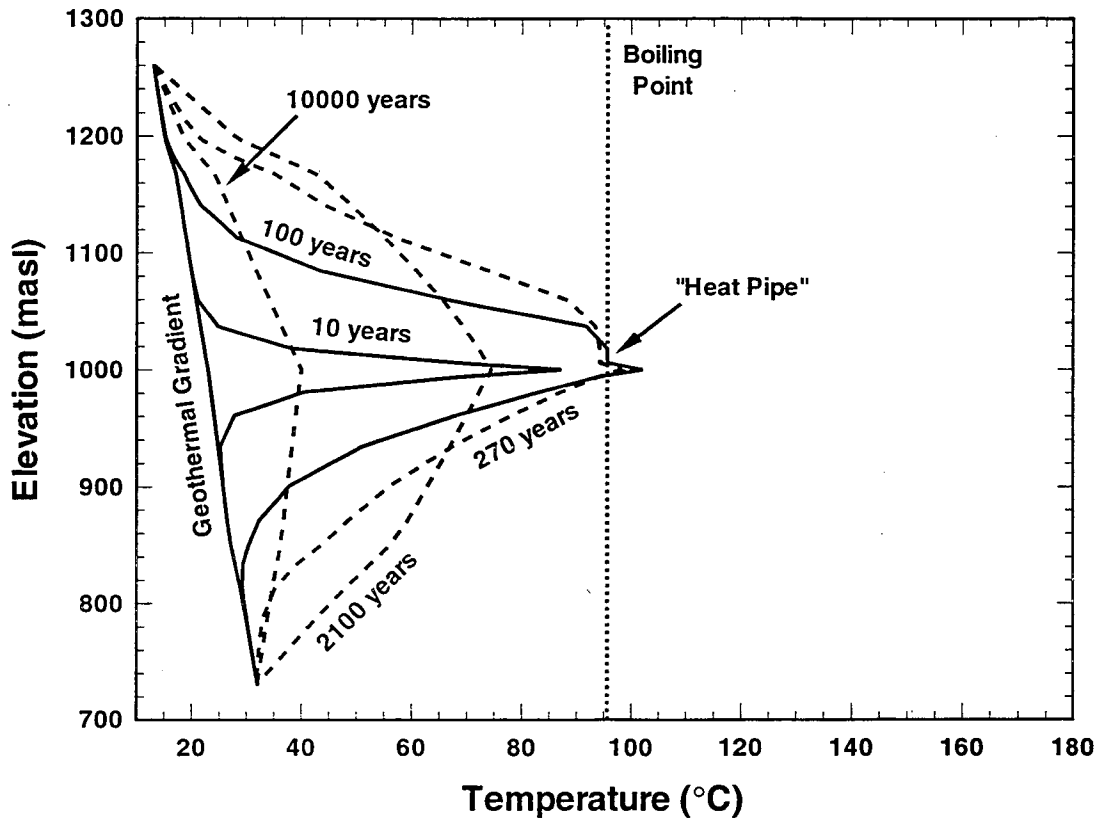


Figure 10.

Vertical temperature profiles along the repository centerline of the eastern emplacement block for APD = 57 kW/acre.

The liquid saturation profiles are given in Figures 11 and 12. Figure 11 shows that a large high-liquid-saturated, condensate zone of about 100 m thick is formed above the repository within the Topopah Spring unit at the time of 100 years under the higher loading condition. For both cases, the vertical saturation profiles, in Figures 11 and 12, will not recover to the starting, ambient condition even in 100,000 years.

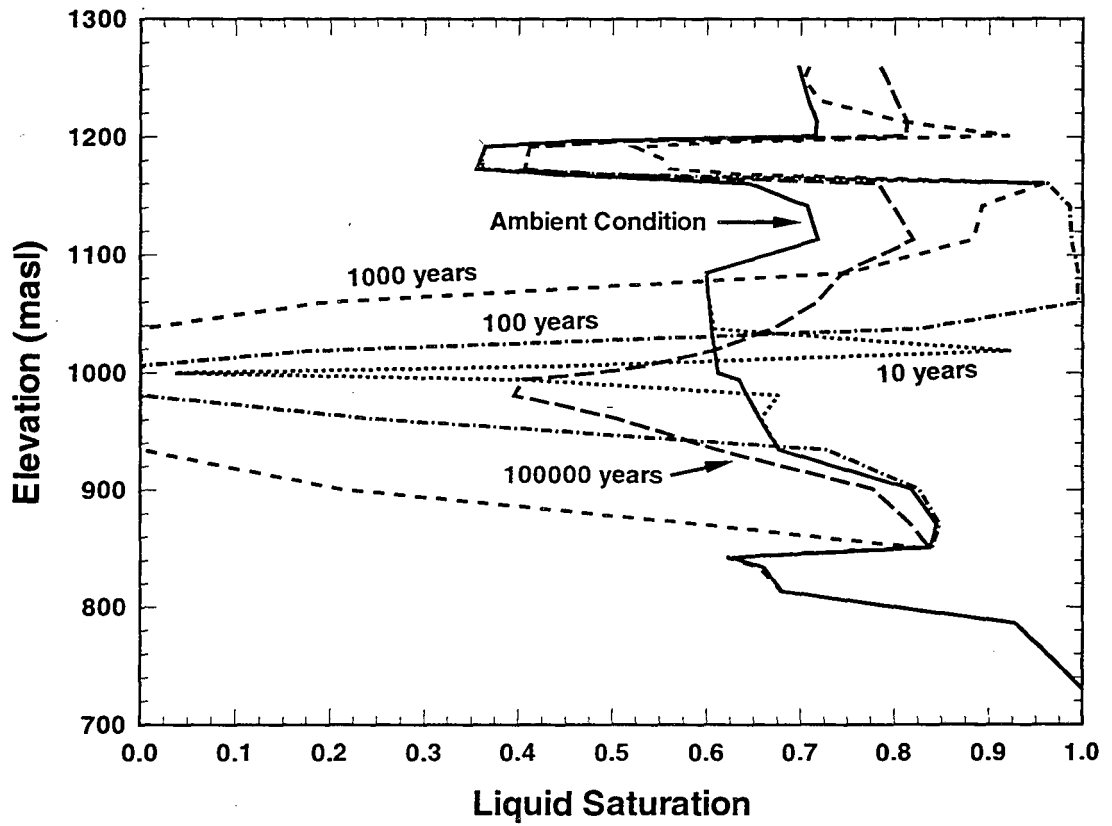


Figure 11.

Vertical saturation profiles along the repository centerline of the eastern emplacement block for APD = 114kW/acre.

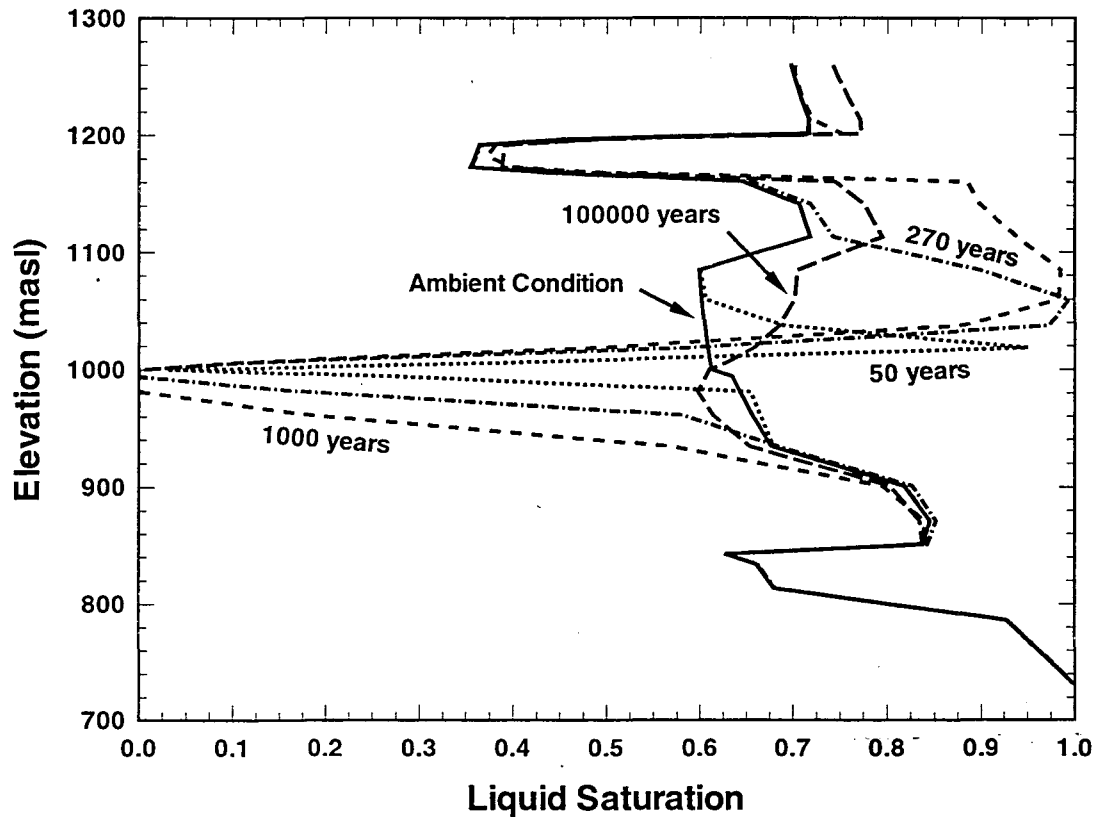


Figure 12.

Vertical saturation profiles along the repository centerline of the eastern emplacement block for APD = 57 kW/acre.

### 3.3 *Effects of Thermal Loadings on Gas and Moisture Flow*

In general, repository heat moves moisture by means of (1) vaporization, (2) driving water vapor from high to low gas-phase pressure zones, (3) condensation, and (4) gravity-capillary driven flow of condensate. The heat transfer and fluid flow are always coupled processes. The physical mechanisms governing heat transfer surrounding a repository include heat conduction and convection (latent and sensible heat flow). Some other minor processes, such as radiation, viscous dissipation and mechanical work, are usually ignored. The



effects of water vaporization and condensation of phase transitions depend upon the local temperature, pressure, vapor pressure, and capillarity conditions.

Figures 13 and 14 show water saturation distributions and associated gas mass flow within the cross-section at a time of 100 years since waste emplacement, and Figures 15 and 16 give the temperature contours and heat flow for the same time. A comparison between Figures 13 and 14, 15 and 16 indicates that much larger dryout zones are generated around the two waste emplacement blocks under the high loading condition. Two relatively higher liquid saturation zones from condensation are created in the dark areas, as shown in Figures 13 and 14, directly above the two repository blocks. For the case of APD = 114 kW/acre, more extensive condensate zones are formed at 100 years, indicating much more rapid two-phase flow rates of repository heat driven vapor and condensate movement around the repository.

Figure 13 and 14 also show the gas mass flow and its distribution for the time of 100 years. The gas flow, or buoyant gas-phase convection, is much more extensive and many orders of magnitude larger around the repository blocks than the ambient conditions, farther away from the waste blocks. The gas (vapor, or steam and air) is driven away from the repository by higher gas pressure generated at the boiling zones. Similarly, the total thermal energy flow from heat conduction and convection, as shown in Figures 15 and 16, at the repository is elevated by many orders of magnitude, moving away from the continuous heat source of the waste packages to the surrounding areas.

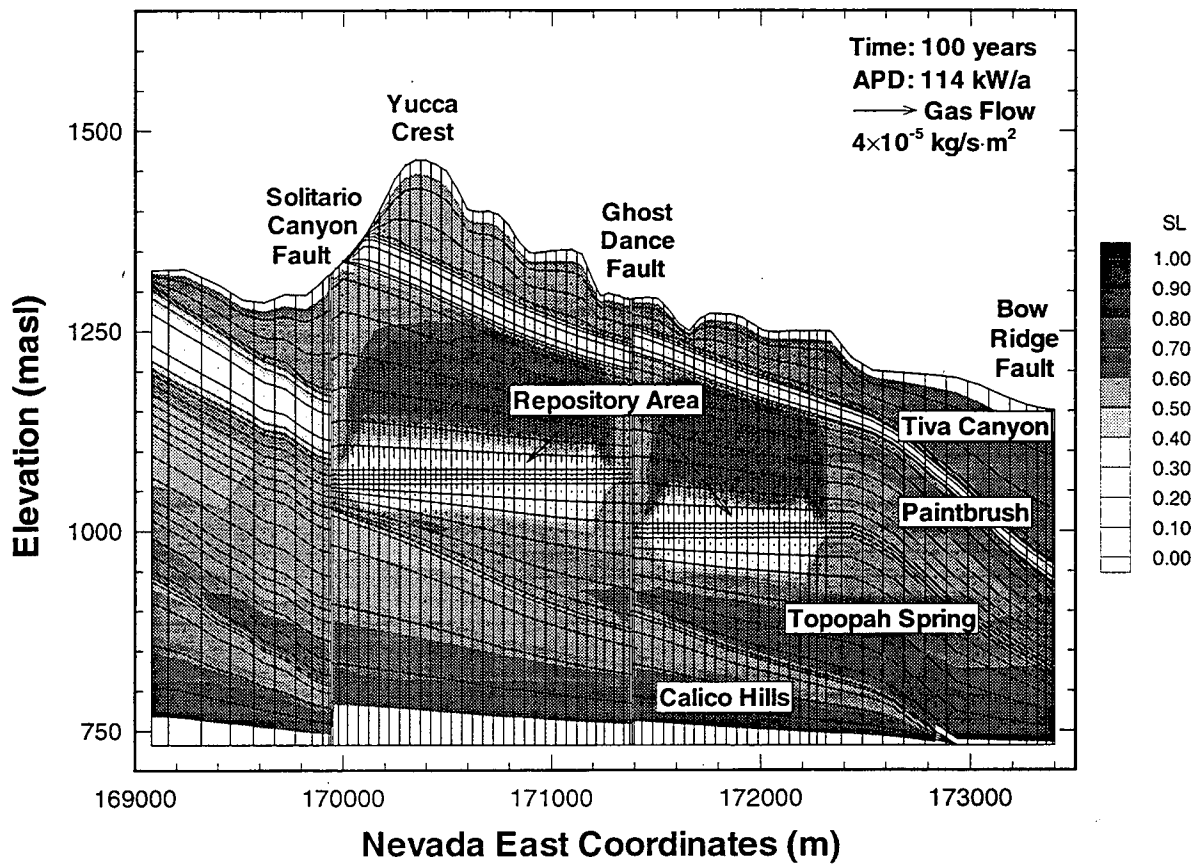


Figure 13.

Liquid saturation distribution and gas flow field at the time of 100 years in the cross-section for APD = 114 kW/acre.

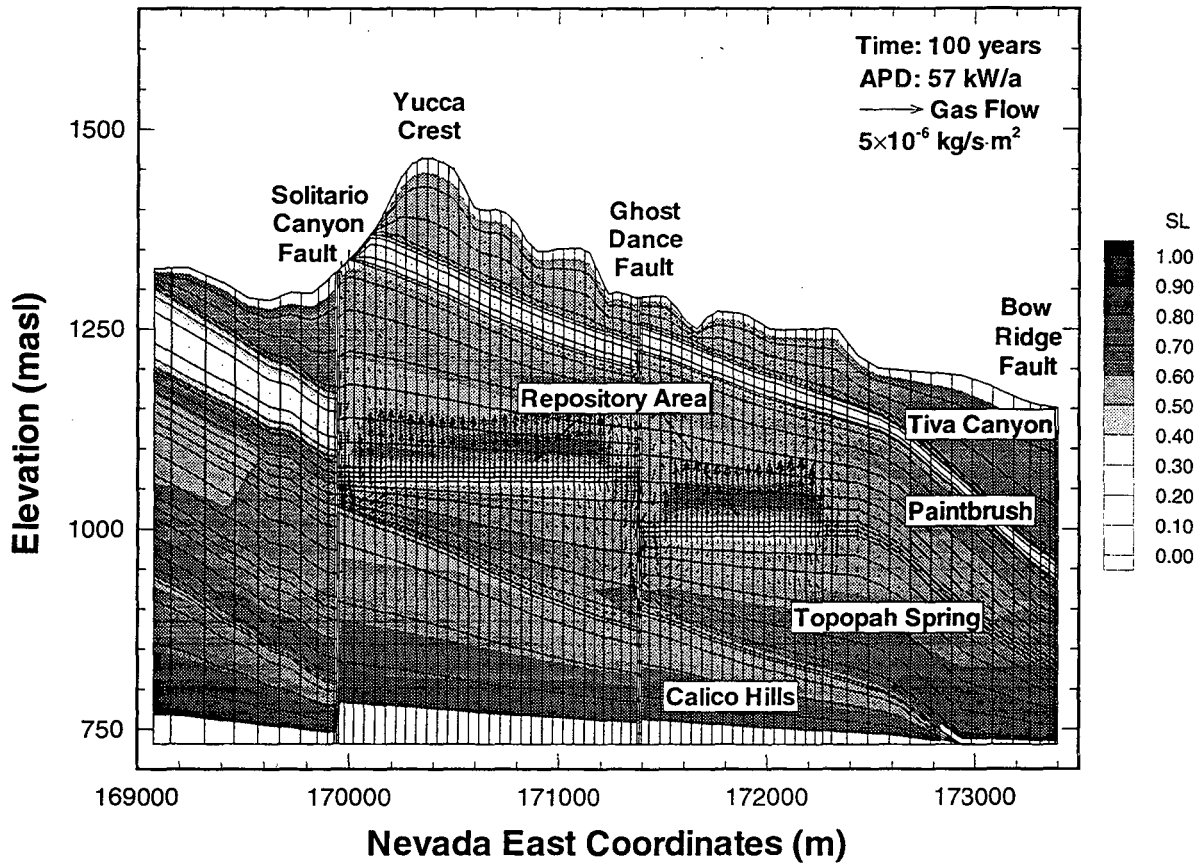


Figure 14.

Liquid saturation distribution and gas flow field at the time of 100 years in the cross-section for APD = 57 kW/acre.

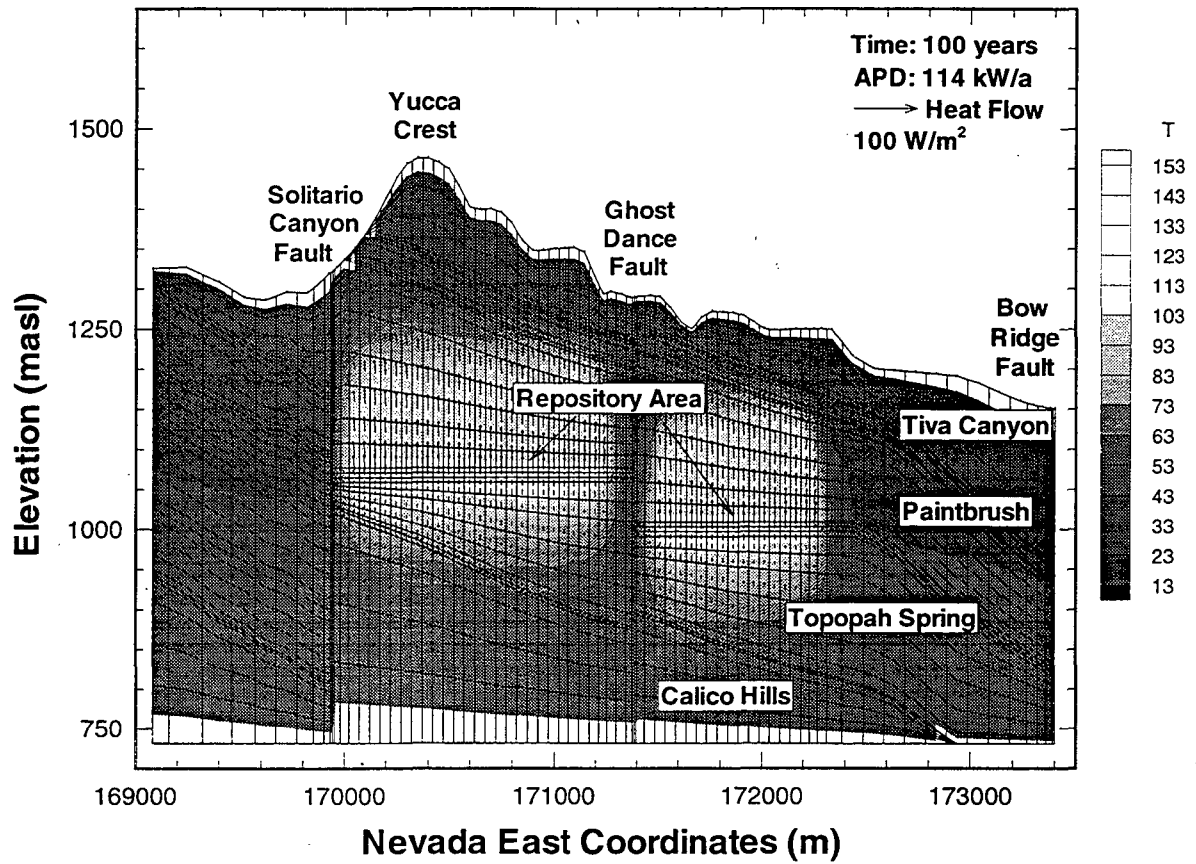


Figure 15.

Temperature distribution and heat flow field at the time of 100 years in the cross-section for APD = 114 kW/acre.

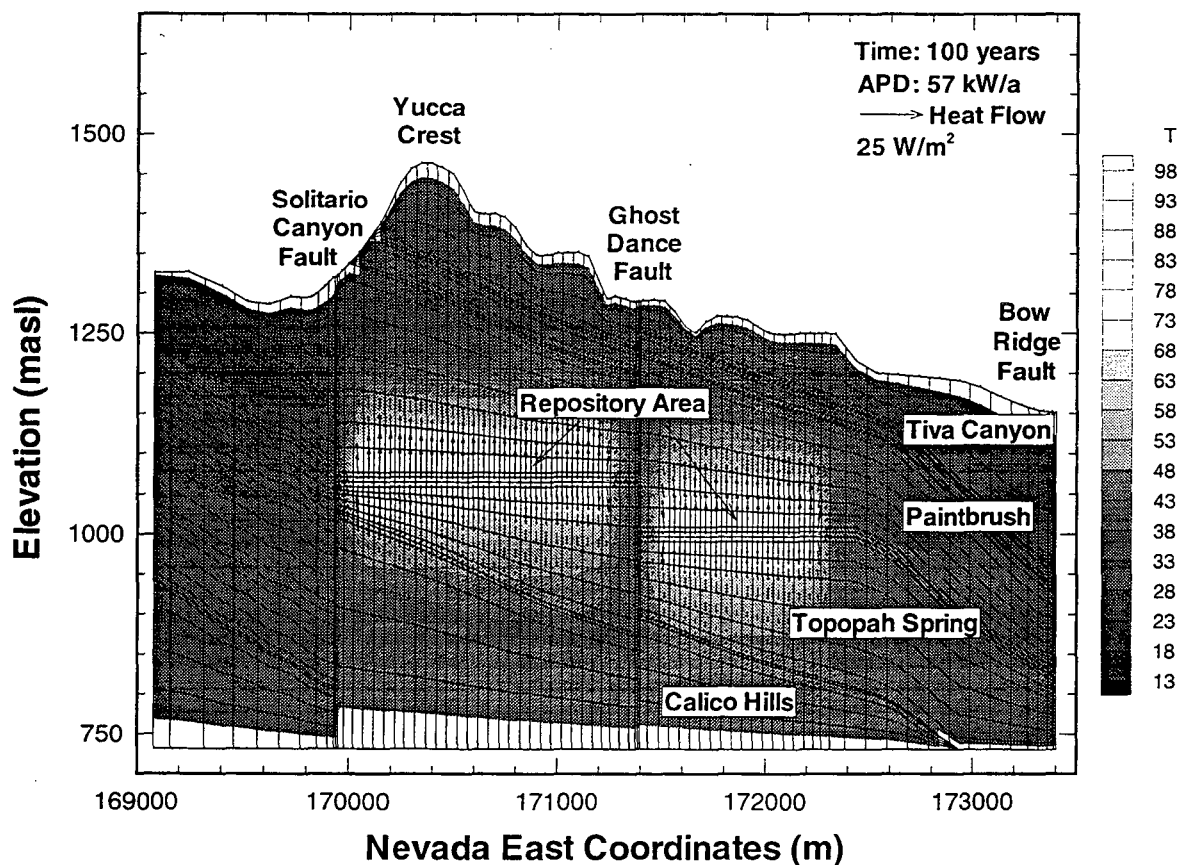


Figure 16.

Temperature distribution and heat flow field at the time of 100 years in the cross-section for APD = 57 kW/acre.

After 1,000 years following waste emplacement, the water saturation and temperature distributions, and gas and heat flow within the cross-section are shown in Figures 17, 18, 19 and 20. Figures 17 and 18 indicate that at this time, both the dryout and the higher gas velocity zones become larger. The high liquid saturation, condensation zones have moved further away from the heat source. It is interesting to note that the Paintbrush unit is partially blocking the gas upflow (see Figures 17 and 18). A large amount of gas flows up and escapes through the Ghost Dance and Solitario Canyon faults, and also through a portion of the Topopah Spring near the Solitario Canyon fault, where both the Tiva

Canyon and the Paintbrush units are missing by erosion and where the Topopah Spring unit is exposed directly to the atmosphere.

The temperature distribution and heat flow at 1,000 years, as shown in Figures 19 and 20, indicate that for both thermal loading scenarios boiling conditions prevail at this time. Much bigger high-temperature zones are created around the repository, compared with those in 100 years. The heat is dissipating from the sources in all directions. Substantial amounts of thermal energy are carried away by flowing gas through the two faults and the exposed area of the Topopah Spring unit near the Solitario Canyon fault.

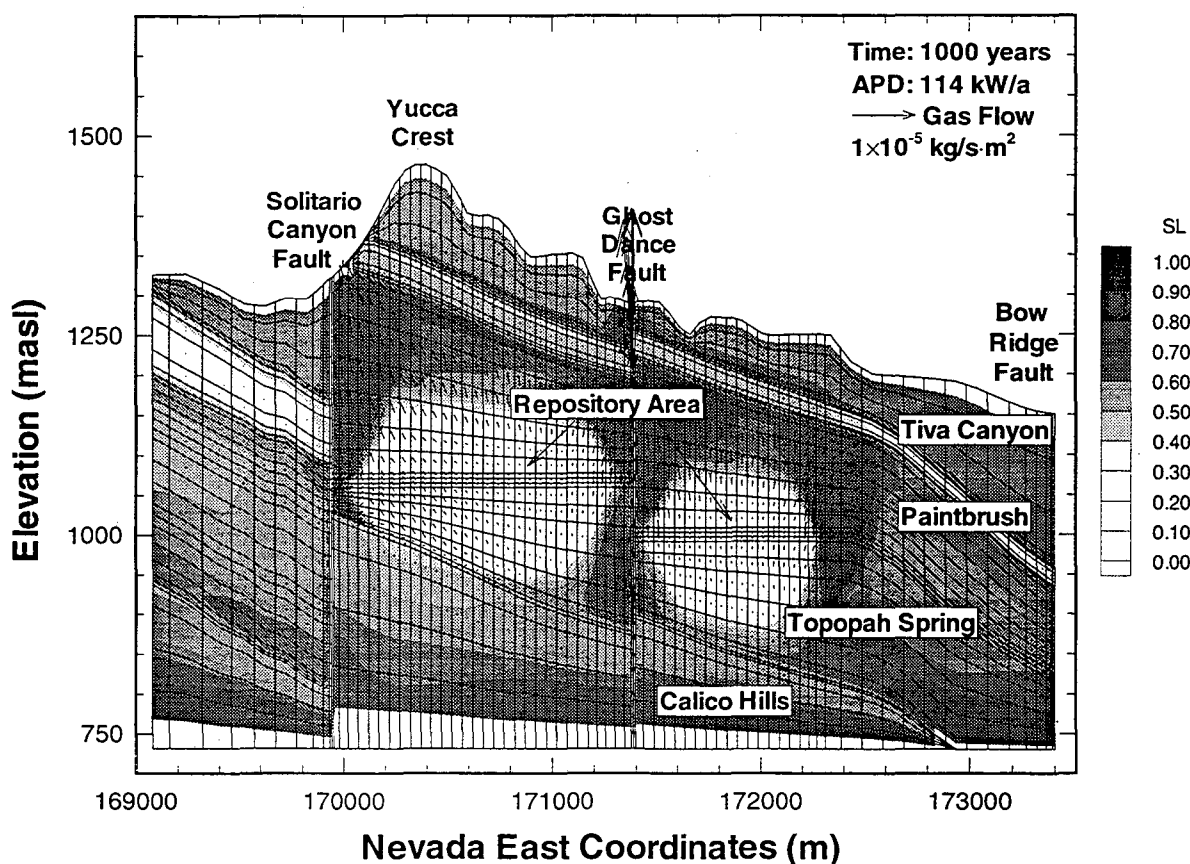


Figure 17.

Liquid saturation distribution and gas flow field at the time of 1000 years in the cross-section for APD = 114 kW/acre.

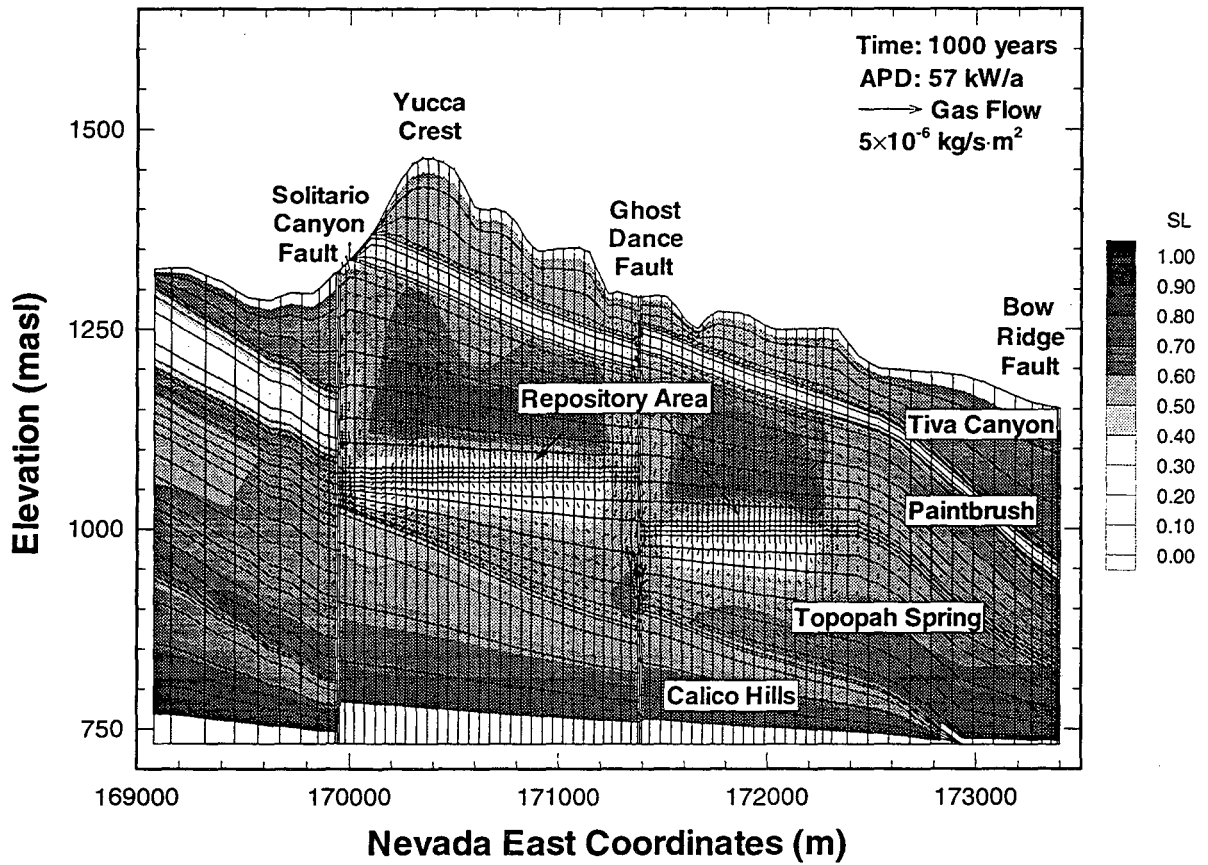


Figure 18.

Liquid saturation distribution and gas flow field at the time of 1000 years in the cross-section for APD = 57 kW/acre.

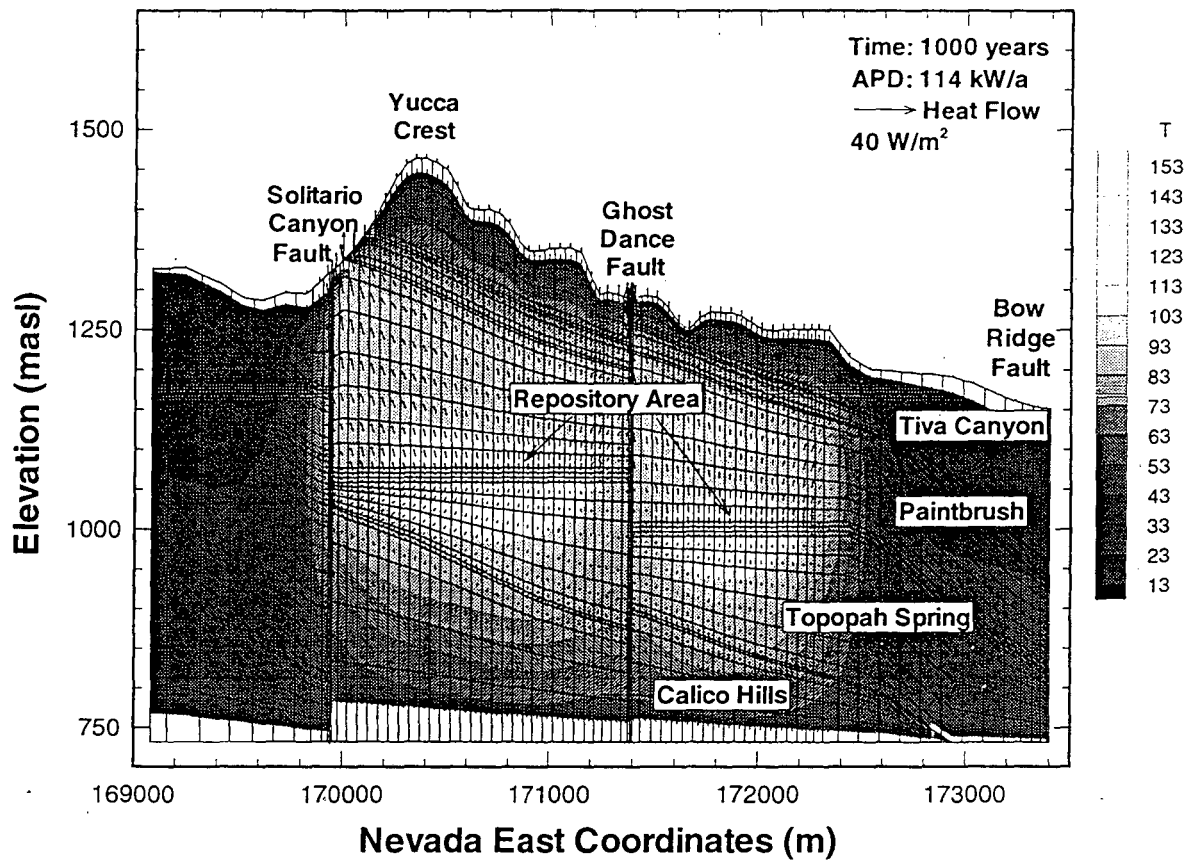


Figure 19.

Temperature distribution and heat flow field at the time of 1000 years in the cross-section for APD = 114 kW/acre.



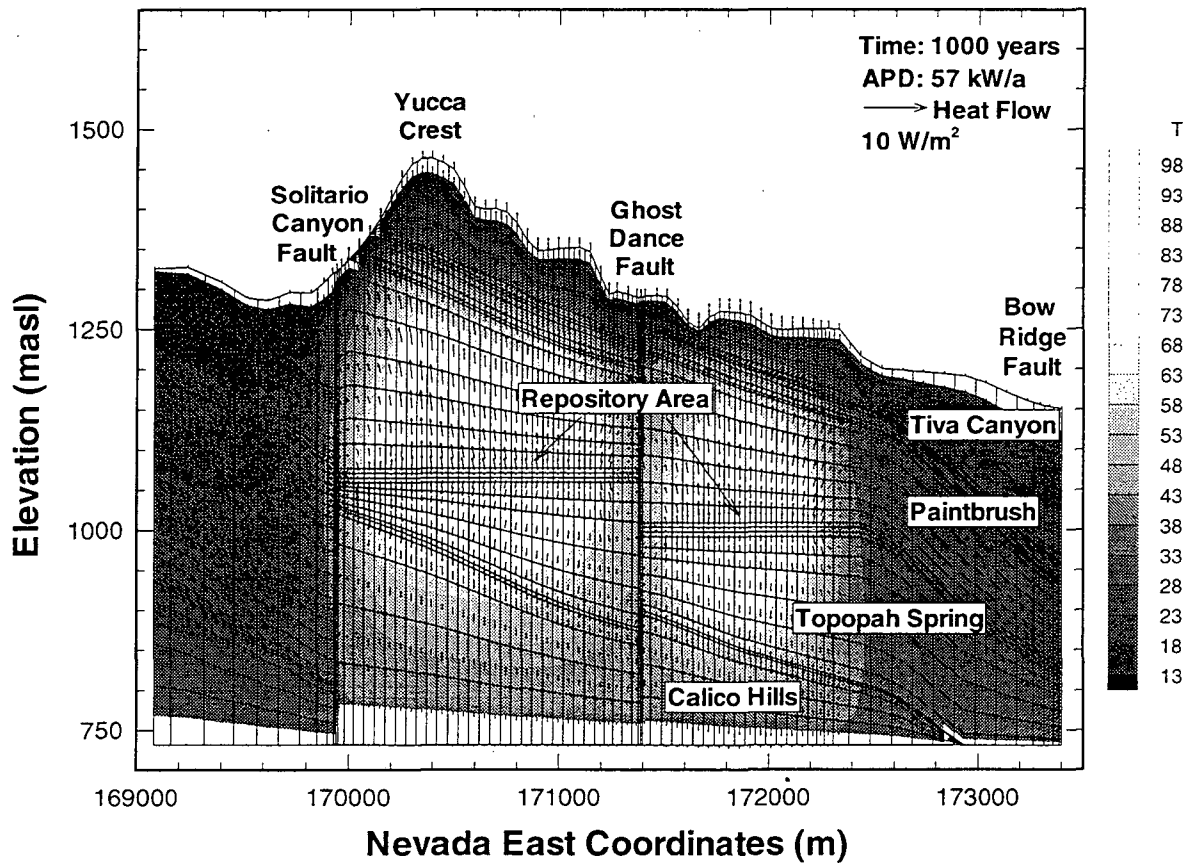


Figure 20.

Temperature distribution and heat flow field at the time of 1000 years in the cross-section for APD = 57 kW/acre.

The elevated gas and heat flow from the underground at Yucca Mountain, associated with the high-level nuclear waste disposal, may have significant impacts on the ecological environment in the surrounding area. The modeling approach has been useful to provide some long-term predictions of the heated gas and heat effluxes from the mountain for a given repository design. Figures 21 and 22 show the surface gas mass fluxes along the cross-section at different

times under the two thermal loading conditions. It is obvious that the gas fluxes increase, and then decrease from their peak values by several orders of magnitude during 10,000 years, as shown in Figures 21 and 22. Most significantly, gas flow through the two faults is increased by more than 4 orders of magnitude, indicating that the faults serve as major pathways for heated gas flow from the mountain.

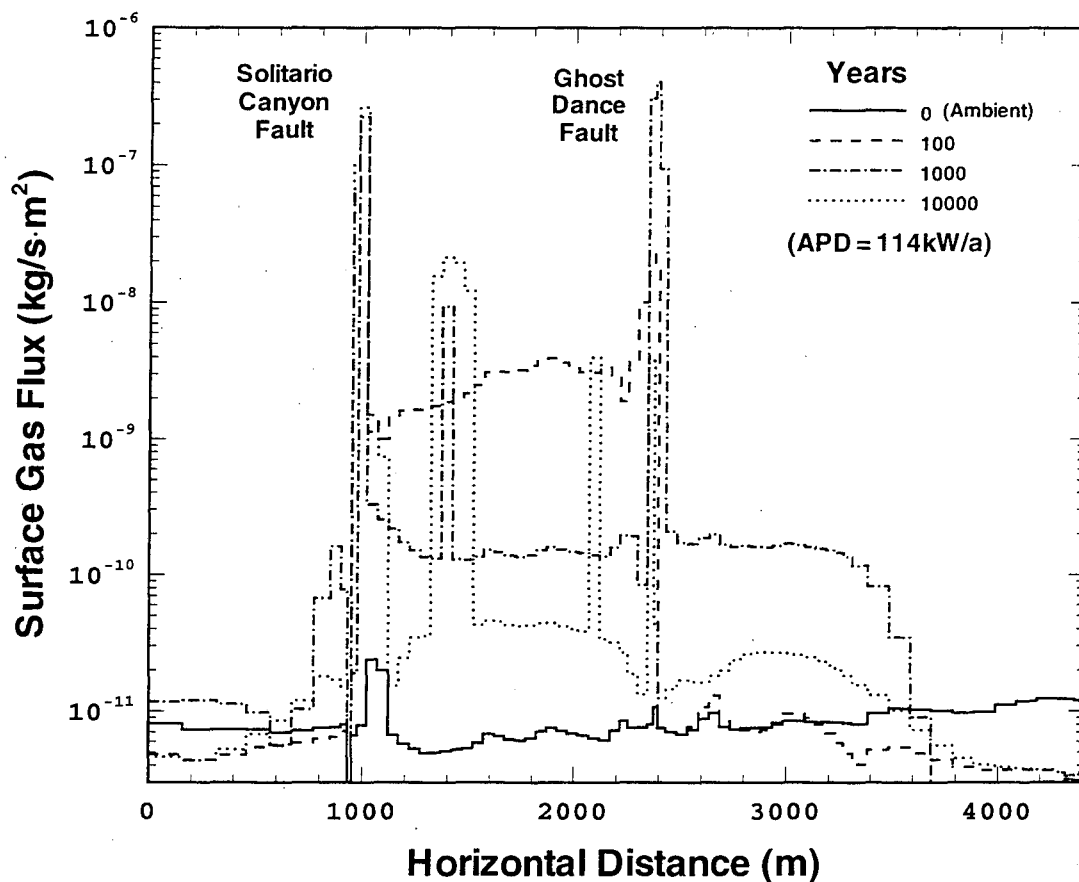


Figure 21.

Surface gas mass flux variations along the cross-section for APD = 114 kW/acre.

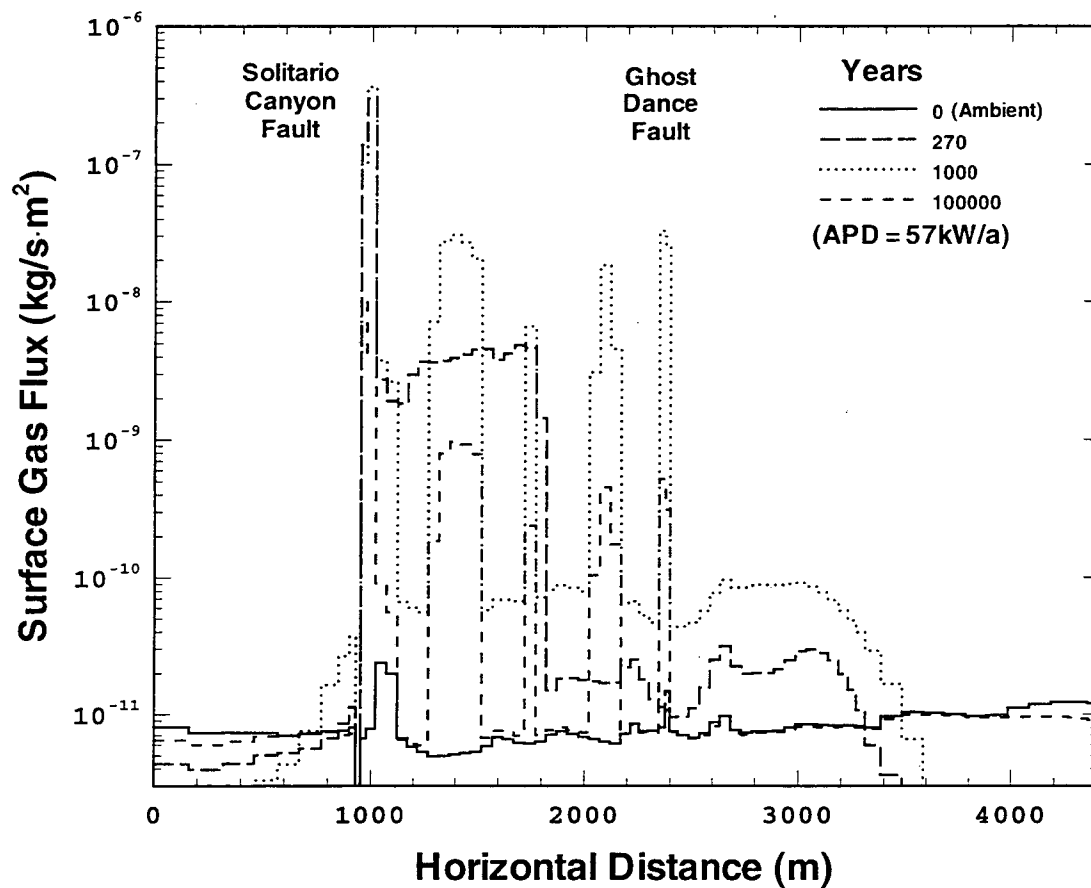


Figure 22.

Surface gas mass flux variations along the cross-section for APD = 57 kW/acre.

The heat flux along the cross-section for different times is shown in Figures 23 and 24, and also increases by 1 to 2 orders of magnitude under the thermal loadings. Figures 23 and 24 indicate that the highest heat flow from the mountain occurs at about 1,000 years, and the faults serve also as main pathways for transferring thermal energy.

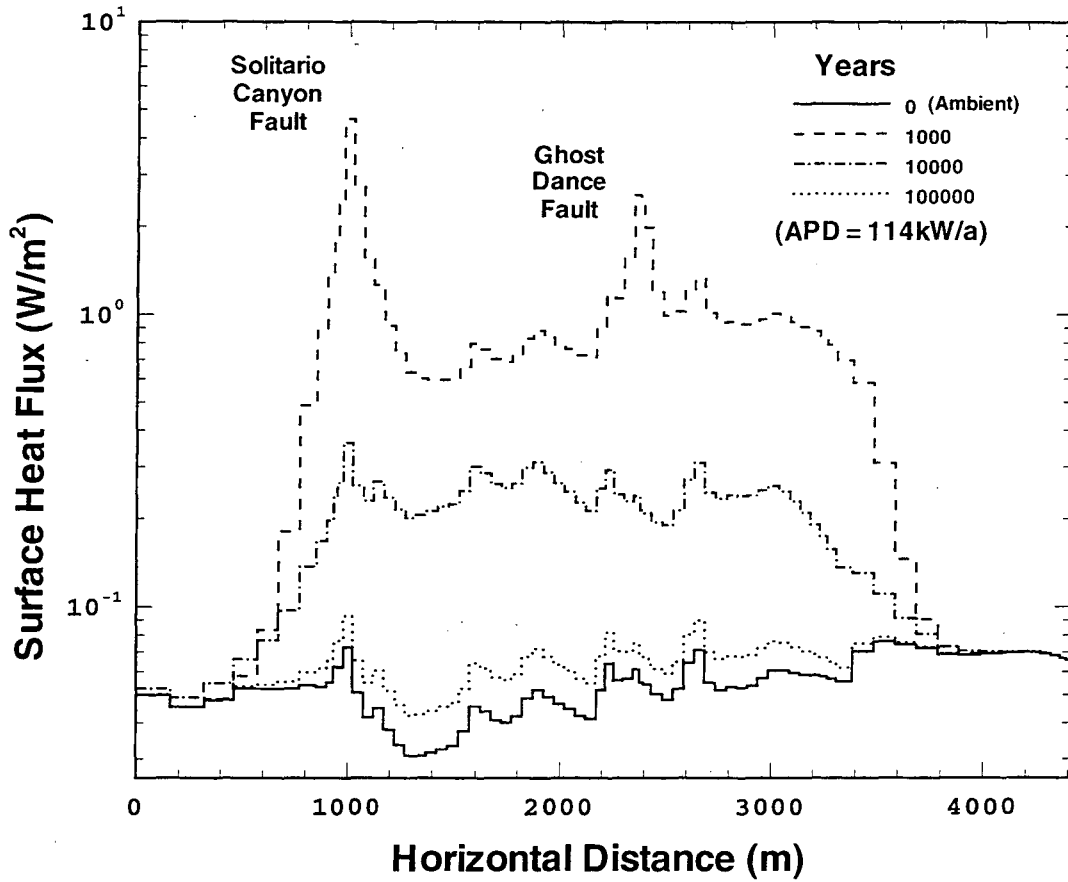


Figure 23.  
 Surface heat flow variations along the cross-section for APD = 114 kW/acre.

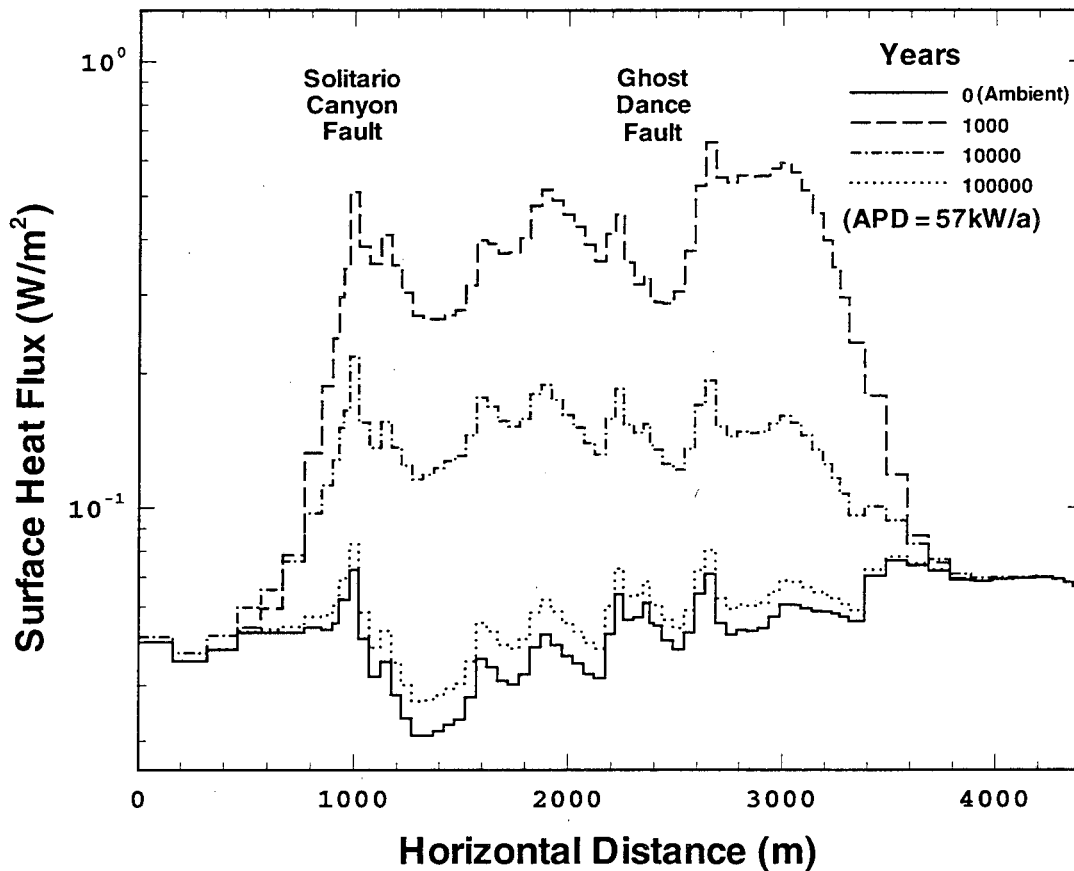


Figure 24.

Surface heat flow variations along the cross-section for APD = 57 kW/acre.

#### 4. CONCLUDING REMARKS

The main objective of this study was to apply the modeling capability of the 3-D site-scale model to evaluating the effects of thermal loading on gas and heat flow at Yucca Mountain, and to provide some insight into the hydrothermal behavior of the unsaturated zone surrounding the repository under thermal loading conditions using more realistic representations of the hydrogeologic system. We are concerned with the spatial variability in rock and fracture properties, including the major fault zones at the site, and their effects on the heated gas

and heat flow through the mountain under the repository thermal loading conditions.

The modeling results presented here are based on numerical simulations using a 2-D vertical cross section of the west-east unsaturated zone from the 3-D LBNL/USGS site-scale model. The 2-D grid for the cross-section includes the variations of different hydrogeologic units along the cross-section, and explicit treatment of major faults, as in the 3-D site-scale model. All the input parameters used for fluid and rock properties were taken from the site-scale model with rock thermal conductivities and heat capacity from RIB (DOE, 1993). Surface and bottom boundary conditions are similar to those for the site-scale model, i.e., constant pressures and temperatures specified. The initial condition corresponds to steady-state condition, with zero net infiltration. At the repository, two thermal loading scenarios are considered: a) APD = 57 kW/acre and b) APD = 114 kW/acre, and the decay thermal source from is ten-year-old mixed waste.

The simulation results indicate that there is a strong influence of thermal loading on the gas and heat flow at the mountain. The averaged surface gas and heat flow is predicted to increase by many orders of magnitude resulting from thermal loading, and the Solitario Canyon fault and the Ghost Dance fault both serve as major pathways for heated gas and heat for the repository layout plan considered. There may be environmental implications for such high heat and gas fluxes which need to be investigated further.

This sensitivity study has demonstrated the potential that significant differences may exist in model predicted temperature and moisture distributions, and heat and gas movement at the mountain, when including the effects of the faults and dipping strata. However, some key properties of the faults and fractures, such as permeability, porosity, capillarity, etc., are not well defined at present. These properties need to be determined for more reliable prediction of the effects of thermal loading on gas, moisture and heat movement in the mountain.

The analysis of the simulation results for thermal loading and its effects on gas and heat flow in the mountain is preliminary, because it was based on a 2-D cross-sectional model and limited simulations. In addition, assumed porous-medium fault properties were used. There is a need for additional 3-D site-scale simulation studies and sensitivity analyses to examine the thermo-hydrologic behavior at the site under possible thermal loadings as more site-specific data become available.

## ACKNOWLEDGMENT

The authors are grateful to Karsten Pruess and Yvonne Tsang for many valuable discussions during this work and for providing decay heat source data. We also thank John Nitao for providing us with many important references on the subject. Thanks are due to Yvonne Tsang and Karsten Pruess for a critical and careful review of the manuscript and for their suggestions for improvements.

## REFERENCES

- Braithwaite, J. W., and F. B. Nimick, Effect of host-rock dissolution and precipitation on permeability in a nuclear waste repository in tuff, Rep. SAN84-0192, Sandia National Laboratory, Albuquerque, NM, Sept. 1984.
- Buscheck, T.A., and J.J. Nitao, Modeling hydrothermal flow in variably saturated, fractured, welded tuff of the Yucca Mountain project, Proceedings of the 5th Workshop Flow and Transport through Unsaturated Fractured Rock, Tucson, Arizona, 1991.
- Buscheck, T.A., and J. J. Nitao, The impact of thermal loading on repository performance at Yucca Mountain, Proceedings Third International High Level Radioactive Waste Management Conference, Las Vegas, NV, April 12-16, 1992.
- Buscheck, T.A., and J. J. Nitao, Repository-heat-driven hydrothermal flow at Yucca Mountain, part I: modeling and analysis, Nuclear Technology, vol. 104, No. 3, pp. 418-448 1993.
- Buscheck, T.A., and J. J. Nitao, The analysis of repository-heat-driven hydrothermal flow at Yucca Mountain, Proceedings, Fourth International High Level Radioactive Waste Management Conference, Las Vegas, NV, April 26-30 1993.
- Buscheck, T.A., and J. J. Nitao, The impact of repository-heat-driven hydrothermal flow on hydrological performance at Yucca Mountain, Proceedings, Fourth International High-Level Radioactive Waste Management Conference, Las Vegas, NV, April 1993. Also, UCRL-JC-112333, Lawrence National Laboratory, Livermore, CA 1993a.

- Buscheck, T.A., and J.J. Nitao, Repository-heat-driven hydrothermal flow at Yucca Mountain, Part I: modeling and analysis, *Nuclear Technology*, vol. 104, No. 3, pp. 449-471, 1993a
- Buscheck, T.A., and J.J. Nitao, Repository-heat-driven hydrothermal flow at Yucca Mountain, Part II: large-scale in situ heater tests, *Nuclear Technology*, vol. 104, No. 3, pp. 418-448 1993b.
- Buscheck, T.A., and J. J. Nitao, The importance of thermal loading conditions to waste package performance at Yucca Mountain, *Proceedings, XVIII International Symposium on the Scientific Basis for Nuclear Waste Management*, Kyoto, Japan, October 23-27, 1994
- Buscheck, T.A., and J.J. Nitao, and D.A. Chesnut, The impact of episodic nonequilibrium fracture-matrix flow on geological repository performance, *Proceedings, American Nuclear Society Topical Meeting on Nuclear Waste Proceedings Packaging (Focus 91)*, Las Vegas, NV, Sept. 30-Oct. 2, 1991. Also, UCRL-JC-106759, Lawrence Livermore National Laboratory, Livermore, CA, 1991.
- Buscheck, T.A., J.J. Nitao, and S.F. Saterlie, Evaluation of thermo-hydrological performance in support of the thermal loading systems study, *Proceedings, International High Level Radioactive Waste Management Conference*, Las Vegas, NV, May 22 -26, 1994.
- M & O, Recommended layout concepts report, BCAA00000-01717-00001, Rev 00, Civilian Radioactive Waste Management System Management and Operating Contractor, Las Vegas, NV, July 1995.
- Mondy, L.A., R.K. Wilson, and N.E. Bixler, Comparison of waste emplacement configurations for a nuclear waste repository in tuff, IV, thermohydrological analysis, Rep. SAND83-0757, Sandia National Laboratory, Albuquerque, NM, Aug. 1983.
- Nielsen, D.R., M.Th. van Genuchten, and J.W. Biggar, Water flow and solute transport in the unsaturated zone, *Water Resources Research*, 22(9), 89S-108S, 1986.
- Nitao, J.J., Numerical modeling of the thermal and hydrological environment around a nuclear waste package using the equivalent continuum approximation: Horizontal emplacement, Rep. UCID-21444, Lawrence Livermore National Laboratory, Livermore, CA, 1988.



- Nitao, J.J., "V-TOUGH, An Enhanced Version of the TOUGH Code for the Thermal and Hydrologic Simulation of Large-Scale Problems in Nuclear Waste Isolation, Rep. UCID-21954, Lawrence Livermore National Laboratory, 1989.
- Nitao, J.J., T.A. Buscheck, and D.A. Chesnut, The implications of episodic nonequilibrium fracture-matrix flow on site suitability and total system performance, Proceedings, Third International High Level Radioactive Waste Management Conference, Las Vegas, NV, April 26-30, 1992.
- Ogniewicz, Y., and C.L. Tien, Porous heat pipe, Heat Transfer Thermal Control and Heat Pipes, Progress in Astronautics and Aeronautics, vol. 70, Martin Summerfield Ser., edited by W.B. Olstad, AAIA, Washington, D.C., 1979.
- Pruess, K., TOUGH user's guide, Nuclear Regulatory Commission Report NUREG/CR-4645; Also Rep. LBL-20700, Lawrence Berkeley Laboratory, Berkeley, CA, 1987.
- Pruess, K., TOUGH2- a general purpose numerical simulator for multiphase fluid and heat flow, Rep. LBL-29400, Lawrence Berkeley Laboratory, Berkeley, CA, May, 1991.
- Pruess, K., and E. Antunez, Application of TOUGH2 to Infiltration of Liquids in Media with Strong Heterogeneity, Proceedings of the TOUGH2 Workshop '95, Lawrence Berkeley Laboratory, Ed., K. Pruess, March, 1995.
- Pruess, K., and T. N. Narasimhan, A Practical Method for Modeling Fluid and Heat Flow in Fractured Porous Media, Soc. Pet. Eng. J., 25(1), p. 14-26.
- Pruess, K., and Y.W. Tsang, Modeling of strongly heat-driven flow processes at a potential high-level nuclear waste repository at Yucca Mountain, Nevada, Proceedings, Fourth International High Level Radioactive Waste Management Conference, Las Vegas, NV, April 26-30, 1993.
- Pruess, K., and Y.W. Tsang, Thermal modeling for a potential high-level nuclear waste repository at Yucca Mountain, Nevada, Rep. LBL-35381 UC-600, Lawrence Berkeley Laboratory, Berkeley, CA, March 1994.

- Pruess, K., and J.S.Y. Wang, TOUGH-A numerical model for nonisothermal unsaturated flow to study waste canister heating effects, in Scientific Basis for Nuclear Waste Management, Mat. Res. Soc. Symp. Proc., vol. 26, edited by G.L. McVay, pp. 1031-1038, Elsevier, NY, 1984.
- Pruess, K., J.S.Y. Wang, and Y.W. Tsang, On thermohydrologic conditions near high-level nuclear wastes emplaced in partially saturated fractured tuff, part I. simulation studies with explicit consideration of fracture effects, Water Resources Res., 26(6), 1235-1248, 1990a.
- Pruess, K., J.S.Y. Wang, and Y.W. Tsang, On the thermohydrologic conditions near high-level nuclear wastes emplaced in partially saturated fractured tuff, part 2. Effective continuum approximation, Water Resources Res., 26(6), 1249-1261, 1990b.
- Ramspott, L.D., The constructive use of heat in an unsaturated tuff repository, Proceedings, Second International High Level Radioactive Waste Management Conference, Las Vegas, NV, April 28-May 2, 1991.
- Ruffner, D., G.L. Johnson, E.A. Platt, J.A. Blink, and T. Doering, Drift emplaced waste package thermal effects, American Nuclear Society, Proceedings Fourth International High-Level Radioactive Waste Management Conference, Las Vegas, NV, April 1993.
- Ryder, E.E., Results of two-dimensional near-field thermal calculations in support of M&O study on repository thermal loading, 1992.
- Travis, B.J. and H.E. Nuttall, Two-dimensional numerical simulation of geochemical transport in Yucca Mountain, Rep. LA10532-MS, Los Alamos National Laboratory, Los Alamos, NM, Dec. 1987.
- Travis, B.J., S.W. Hodson, H.E. Nuttall, T.L. Cook, and R.S. Rundberg, Numerical simulation of flow and transport in fractured tuff. Mat. Res. Soc. Symp. Proc., vol. 26, pp. 1039-1047, Elsevier, NY, 1984.
- Tsang, Y.W., and K. Pruess, A study of thermally induced convection near a high-level nuclear waste repository in partially saturated fractured tuff, Water Resources Research, 23 (10), 1958-1966, 1987.

- Udell, K.S., Heat transfer in porous media considering phase change and capillarity - the heat pipe effect, *Int. J. Heat Mass Transfer*, 28(2), 485-195, 1985.
- U. S. Department of Energy (DOE), Yucca Mountain Site Characterization Project, Reference Information Base (RIB), OCRMW, YMP/93-02, Rev. 3, 1993.
- Wilder, D.G., Alternative strategies-a means for saving money and time on the Yucca Mountain project, *Proceedings, Fourth International High Level Radioactive Waste Management Conference*, Las Vegas, NV, April 26-30, 1993.
- Wittwer, C., G. Chen, G.S. Bodvarsson, M. Chornack, A. Flint, E. Kwicklis, and R. Spengler, The development of the LBL/USGS three-dimensional site-scale model of Yucca Mountain, Nevada, *Research Report*, Lawrence Berkeley Laboratory, Berkeley, California, 1994.
- Wittwer, C., G. Chen, G.S. Bodvarsson, M. Chornack, A. Flint, E. Kwicklis, and R. Spengler, Preliminary development of the LBL/USGS three-dimensional site-scale model of Yucca Mountain, Nevada, *Research Report LBL-37356, UC-814*, Lawrence Berkeley National Laboratory, Berkeley, California, 1995.
- Zimmerman, R.M., First phase of small diameter heater experiments in tuff, *Proceedings, 27th U.S. Symposium on Rock Mechanics*, Texas A&M University, College Station, TX, June 1983.
- Zimmerman, R.M., and M. L. Blanford, Expected thermal and hydrothermal environments for waste emplacement holes based on G-tunnel heater experiments, *Proceedings, 27th U.S. Symposium on Rock Mechanics*, pp. 874-882, 1986.
- Zimmerman, R.M., F.B. Nimick, and M.B. Board, Geoengineering characterization of welded tuffs from laboratory and field investigations, *Mat. Res. Soc. Symp. Proc.*, vol. 44, pp. 547-554, Materials Research Society, Pittsburgh, PA, 1995a.

**FIGURES:**

- Figure 1. A plan view of the potential repository at Yucca Mountain, showing the two waste emplacement blocks, major faults, the cross-section, and the site-scale model domain.
- Figure 2. Grid of the 2-D west-east cross-section along the Nevada Coordinates N 233000.
- Figure 3. The initial distribution of liquid saturation in the cross-section.
- Figure 4. The initial distribution of temperature in the cross-section.
- Figure 5. Variations in temperature and saturation at the center of the eastern emplacement block for APD = 114 kW/acre.
- Figure 6. Variations in temperature and saturation at the center of the eastern emplacement block for APD = 57 kW/acre.
- Figure 7. Temperature increases near the ground surface above the repository for APD = 114 kW/acre.
- Figure 8. Temperature increases near the ground surface above the repository for APD = 57 kW/acre.
- Figure 9. Vertical temperature profiles along the repository centerline of the eastern emplacement block for APD = 114 kW/acre.
- Figure 10. Vertical temperature profiles along the repository centerline of the eastern emplacement block for APD = 57 kW/acre.
- Figure 11. Vertical saturation profiles along the repository centerline of the eastern emplacement block for APD = 114kW/acre.
- Figure 12. Vertical saturation profiles along the repository centerline of the eastern emplacement block for APD = 57 kW/acre.
- Figure 13. Liquid saturation distribution and gas flow field at the time of 100 years in the cross-section for APD = 114 kW/acre.

- Figure 14. Liquid saturation distribution and gas flow field at the time of 100 years in the cross-section for APD = 57 kW/acre.
- Figure 15. Temperature distribution and heat flow field at the time of 100 years in the cross-section for APD = 114 kW/acre.
- Figure 16. Temperature distribution and heat flow field at the time of 100 years in the cross-section for APD = 57 kW/acre.
- Figure 17. Liquid saturation distribution and gas flow field at the time of 1000 years in the cross-section for APD = 114 kW/acre.
- Figure 18. Liquid saturation distribution and gas flow field at the time of 1000 years in the cross-section for APD = 57 kW/acre.
- Figure 19. Temperature distribution and heat flow field at the time of 1000 years in the cross-section for APD = 114 kW/acre.
- Figure 20. Temperature distribution and heat flow field at the time of 1000 years in the cross-section for APD = 57 kW/acre.
- Figure 21. Surface gas mass flux variations along the cross-section for APD = 114 kW/acre.
- Figure 22. Surface gas mass flux variations along the cross-section for APD = 57 kW/acre.
- Figure 23. Surface heat flow variations along the cross-section for APD = 114 kW/acre.
- Figure 24. Surface heat flow variations along the cross-section for APD = 57 kW/acre.

LAWRENCE BERKELEY NATIONAL LABORATORY  
UNIVERSITY OF CALIFORNIA  
TECHNICAL & ELECTRONIC INFORMATION DEPARTMENT  
BERKELEY, CALIFORNIA 94720